sustainability

MDPI

Article

Tracing Methanogenesis Pathways via Stable Carbon Isotopes for Sustainable Biogas Production in Continuous-Flow Open Systems

Michał Bucha [1,*], Anna Detman-Ignatowska [2], Aleksandra Chojnacka [2,3], Ewa Łupikasza [4], Łukasz Pleśniak [1], Wojciech Drzewicki [1], Marta Jakubiak [1], Adriana Trojanowska-Olichwer [1], Beata Berbeć [1], Dominika Kufka [5], Anna Sikora [2] and Mariusz Orion Jędrysek [1]

[1] Institute of Geological Sciences, University of Wroclaw, Max Born Sq. 9, 50-204 Wrocław, Poland; lukasz.plesniak@uwr.edu.pl (Ł.P.); wojciech.drzewicki@uwr.edu.pl (W.D.); marta.jakubiak@uwr.edu.pl (M.J.); adriana.trojanowska-olichwer@uwr.edu.pl (A.T.-O.); beatamonikabiega@gmail.com (B.B.); mariusz.jedrysek@uwr.edu.pl (M.O.J.)
[2] Institute of Biochemistry and Biophysics, Polish Academy of Sciences, Pawińskiego 5A, 02-106 Warszawa, Poland; annadetman@ibb.waw.pl (A.D.-I.); aleksandra_chojnacka@sggw.edu.pl (A.C.); annaw@ibb.waw.pl (A.S.)
[3] Institute of Biology, Warsaw University of Life Sciences, Nowoursynowska 159, 02-776 Warszawa, Poland
[4] Institute of Earth Sciences, University of Silesia, Będzinska 60, 41-200 Sosnowiec, Poland; ewa.lupikasza@us.edu.pl
[5] "Poltegor–Instytut" Opencast Mining Institute, Parkowa 25, 51-616 Wrocław, Poland; dominika.kufka@igo.wroc.pl
* Correspondence: michal.bucha@uwr.edu.pl

Abstract

The common products of acidogenesis, the key stage in the process of anaerobic digestion, are lactate, butyrate, propionate, and acetate. They were decomposed in the Up-flow Anaerobic Sludge Blanket bioreactors working in continuous-flow open systems. A comprehensive analysis of variations in both isotopic ratios and concentrations of organic acids in the effluents was conducted to enhance comprehension of methanogenic processes. The analysis of carbon isotope fractionation in the CO_2-CH_4 system, as evidenced by the $\alpha^{13}C_{CO2\text{-}CH4}$ factor, has indicated that acetate decarboxylation has occurred. Furthermore, a decline in CO_2 levels was observed, accompanied by the predominance of butyrate and propionate, despite the presence of acetic acid in the effluents from all the bioreactors. Butyric acid demonstrated the greatest resistance to decomposition, resulting in ^{13}C-enrichment of DIC. Lactic acid was utilised almost entirely. The observations presented above were subsequently validated through statistical analysis. A comparative analysis of the $\delta^{13}C(CH_4)$ and $\delta^{13}C(CO_2)$ values of our study with those of other natural substrates (detritic lignite, xylite, maize silage, and cattle manure) was undertaken, and it was found that isotope fractionation differs significantly in closed (potential thermodynamic processes) and open systems (expected Rayleigh processes). In the context of open systems, the isotope fractionation factor $\alpha^{13}C_{CO2\text{-}CH4}$ during methaneogenesis has been observed to attain values that are consistent with those observed in CH_4 oxidation. The study revealed that the presence of acetate in the substrate (i.e., the M4 bioreactor) led to the generation of CO_2 with a higher proportion of light carbon isotopes. This, in turn, resulted in a shift in the isotope fractionation factor (i.e., $\alpha^{13}C_{CO2\text{-}CH4}$) to values below 1.03. Our results suggest that methanogenic pathway signatures in open, continuous-flow systems may only be partially apparent. This is because substrate depletion drives Rayleigh-type isotope enrichment, while the dominance of a single substrate and its constant inflow stabilise pathway expression and shift control towards substrate dynamics rather than intrinsic microbial changes. Our finding suggests that isotope-based diagnostics could enhance

Check for updates

Academic Editors: Jiho Yoo and Hokyung Choi

Received: 5 May 2026
Revised: 26 June 2026
Accepted: 29 June 2026
Published: 6 July 2026

Copyright: © 2026 by the authors. Licensee MDPI, Basel, Switzerland. This article is an open access article distributed under the terms and conditions of the Creative Commons Attribution (CC BY) license.

process control in biogas plants by identifying substrate-driven limitations and facilitating more efficient and stable CH_4 production.

Keywords: substrate-dominated methanogenesis; continuous-flow open systems; isotope-based process monitoring; sustainable biogas production; methanogenic pathways in engineered systems

1. Introduction

Anaerobic biogeochemical processes are widespread in organic-rich natural environments, e.g., marine and freshwater sediments, wetlands, marshes, peat, and coal beds. Methanogenesis represents the final stage of anaerobic decomposition of organic matter. The enhancement of comprehension pertaining to the process of biogas production from organic substances, encompassing organic, industrial/municipal, and agricultural waste, is of paramount significance to the energy industry. Therefore, stimulation of methanogenic processes is crucial for efficient utilisation of any organic wastes, organic-rich sediments, and microbial production of coal-bed methane (MCBM) [1–5].

Microbial CH_4 is synthesised by a narrow group of microorganisms, methanogenic *Archaea*, from strictly defined substrates (namely acetate, formate, hydrogen, and carbon dioxide; methyl compounds, and alcohols). In the natural environment, the most common methanogenesis pathways are as follows: CO_2 reduction, acetate fermentation, and reduction of the methyl groups in methylated compounds (e.g., methanol, methylated amines, and methylated sulphides). Methanogenesis is also possible by direct cleaving off methoxy group of coal macromolecules [6], which is especially important when considering the formation of MCBM. The main factors limiting CH_4 formation are the presence of competing electron acceptors (e.g., nitrates and sulphates) and free oxygen [7–10].

The molecular-level analysis of methanogenic pathways can be facilitated by means of stable isotopic analysis of carbon and hydrogen in a substrate–product system. Biodegradation processes are accompanied by isotope effects, whereby lighter isotopes of the same substance generally react more rapidly than heavier isotopes. This results in the lighter isotopes being partitioned to the reduced form compounds. The isotopic composition of any substance is determined by the isotopic composition and abundance of its sources, the mechanisms of its formation, and the temperature. Thus, in the natural environment, every substance has a specific isotopic signature defined by a delta (δ) value [11–14].

Microbial CH_4 formation via the CO_2 reduction pathway and H_2 oxidation shows lower $\delta^{13}C$ values in the range of −110 to −60‰ [15,16], compared to acetic acid decarboxylation from −60 to −33‰ [17,18]. Carbon isotope analysis is a reliable method of tracing the sources and mechanisms of biodegradation through a combination of laboratory experiments [9]. The majority of these mechanisms have been derived from spatial and temporal variations in the isotopic composition of CH_4 and CO_2 in situ [19]. The combined $\delta^{13}C(CH_4)$ and $\delta^{13}C(CO_2)$ values in biogas from incubation experiments allow for calculation of the potential isotopic fractionation factor of $\alpha^{13}C_{CO2\text{-}CH4}$. This is according to the following equation: $\alpha^{13}C_{CO2\text{-}CH4} = (\delta^{13}C(CO_2) + 1000)/(\delta^{13}C(CH_4) + 1000)$ [20]. The range of values for $\alpha^{13}CCO_2\text{-}CH_4$ typically observed in the context of CO_2 reduction falls within the range of 1.049–1.095. Similarly, the range of values for acetate decarboxylation typically observed is 1.039–1.058. Finally, the range of values for CH_4 oxidation typically observed is 1.005–1.03 [1,18,21,22].

Studies of isotope fractionation between CH_4 and CO_2 during methanogenesis are primarily based on laboratory experiments in which pure microbial cultures are applied

in CO_2 reduction [23–26] or acetate fermentation [18,27,28]. The carbon stable isotopes in dissolved inorganic carbon ($\delta^{13}C(DIC)$) are typically analysed in field studies of groundwaters and surface waters, but less often in a laboratory setting [8,29]. However, $\delta^{13}C(DIC)$ variations help to quantitatively assess the mixing ratios of inorganic carbon of diverse origin and redox processes, including microbial mineralisation of organic substrates. Meister and Reyes [30] showed that the isotopic difference between DIC and CH_4 is often near the thermodynamic equilibrium on the order of 75 ‰. The $\delta^{13}C(CH_4)$ variations are usually a result of anaerobic digestion, while traditionally monitored parameters (pH, VFAs, and VOA/TIC) exhibit a change some five to ten days later [31].

In a laboratory setting, the process of carbon isotope fractionation is determined by the isotopic composition of carbon nutrients (e.g., reduction of CO_2 decreases substrate concentration with simultaneous $^{12}CO_2$ depletion, increasing the $^{13}C/^{12}C$ ratio in the residual DIC), multi-stage decomposition, and oxidation of CH_4 and other biological (e.g., changes in metabolic pathways) and chemical processes (e.g., using different sources of organic carbon) [13,32–34]. Under laboratory conditions, many of these factors can be controlled, allowing overlapping or contradicting factors to be eliminated or constrained. The application of ^{13}C-labelled substrates enables tracing of biodegradation mechanisms and products due to significant enrichment in heavy isotopes of carbon in some products [18]. Consequently, this helps to qualitatively and often quantitatively understand complex environmental processes. Isotopic mass balance offers a reliable tool to quantitatively assess the rate of various, even competitive, processes, such as biodegradation.

The focus of microbiological studieson anaerobic microbiomes, interactions within microbial communities, and the assignment of functions to specific microbial groups during the decomposition of organic matter. This research area is of particular interest due to the role of these microbiomes in methanogenic processes. The factors influencing biogeochemical processes are interactions in microbial communities, feedstock types, stoichiometry, and operational conditions such as temperature, pH, bioreactor construction, organic loading rate, hydraulic retention time, etc. It is evident that these factors have a profound impact on the structure of microbiomes, serve to determine the methanogenic pathway, and exert a significant influence on CH_4 yield [35].

In a previous study, the focus was on a set of four CH_4-producing microbial communities that had been fed an artificial medium which was designed to mimic acidogenic products, focusing on how dominant components—i.e., lactate, butyrate, propionate, and acetate—influenced bioreactor performance, microbial composition, potential, and function [36,37]. It was demonstrated that the acetotrophic pathway of CH_4 formation is determined by lactate and acetate, whereas the contribution of the hydrogenotrophic pathway is increased by butyrate and propionate [38], thereby highlighting the importance of common acidogenic products in determining the metabolic pathways of CH_4 formation. The analysis of lactate, acetate, propionate, and butyrate metabolism is of particular importance, as these compounds represent key intermediate metabolites in anaerobic digestion pathways leading to CH_4 production. Organic biomass is ultimately converted into these volatile fatty acids, which serve as key intermediates and are further transformed into direct substrates for methanogens, leading to methane production. Analysis of these pathways provided insight into the metabolic routes and microbial interactions occurring during acetogenesis and methanogenesis. These processes are fundamental to the carbon cycle and occur in both natural and anthropogenic environments.

Here, we focus on an in-depth C-isotopic analysis of CH_4, CO_2, and DIC present during the conversion of butyrate, propionate, lactate, and acetate to CH_4 by anaerobic microbial communities. Such insights are important to monitor the biochemical reactions during organic matter decomposition and process stability, and to accurately identify the

adaptability of microorganisms to various typical organic carbon sources. The presented results are important for industry (as they provide valuable knowledge about methanogenesis under conditions of continuous substrate availability) and their application in environmental research. This work underscores the potential of isotope-based diagnostics to refine process control in biogas plants by revealing substrate-driven constraints, enabling more efficient and stable CH_4 production.

2. Materials and Methods

2.1. Experimental Setup

Four CH_4-yielding microbial communities (M1, M2, M3, and M4) were cultivated in 3.5 L Up-flow Anaerobic Sludge Blanket (UASB) bioreactors (custom-designed and constructed in-house by the authors at Institute of Biochemistry and Biophysics, Polish Academy of Sciences, Warszawa, Poland). These bioreactors were inoculated with anaerobic sludge and artificial media. Activated sludge was collected from a municipal waste treatment plant "Warszawa Południe" in Warszawa, Poland. The artificial medium used in this study was a modified M9 medium (BD Diffco) without the addition of $MgSO_4$, $CaCl_2$, and glucose. In each bioreactor, methanisation of the predominant products of four different types of acid fermentation proceeded—lactic (M1), butyric (M2), propionic (M3), or acetic acid (M4).

In summary, at the initial stage of the experiment, 1.5 L of activated sludge was combined with 2.0 L of the artificial M9 medium (pH = 7) and then subjected to incubation within the UASB bioreactors for a period of two weeks at ambient temperature (20–25 °C). On the 17th day of the experiment, the media composition was found to contain a mixture of organic salts, with a predominance of one constituent reaching 70%. The continuous supply of this mixture to the UASB bioreactors was initiated using a peristaltic pump (type PP1 B-05, ZALIMP, Warszawa, Poland), with a hydraulic retention time of one week. The UASB bioreactors operated under these conditions till 108 weeks of incubation.

Additionally, during the 45th week of incubation, 500 mL of the microbial consortia was removed from each of the UASB reactors and re-filled with 500 mL of CH_4-yielding sludge from another 50 L-UASB bioreactor containing acidic effluent from molasses fermentation. The aim of this treatment was to refresh the inoculum that had previously been used for testing and optimising the experimental conditions. The sludge used originally came from the same source as the initial inoculum used in the bioreactors.

The total time of incubation was 128 weeks (896 days), during which two experimental sessions (Experiment 1 and Experiment 2) were carried out. Experiment 1 (102–108 weeks) was carried out using artificial media containing a mixture of organic salts with 70% domination of one salt. During Experiment 2 (115–128 weeks), media transferred to the UASB bioreactors contained a single organic salt. Due to limitations in available laboratory space and equipment, it was not feasible to perform the experiment with multiple biological replicates. We are aware that this is a limitation. At the stage of conducting the experiment, we did not plan to perform compound-specific isotope analyses. The goal of this work was to obtain as much information as possible in continuous cultures, so any additional modifications would require separate experimental series. Such experiments should be repeated in large numbers, preferably in batch bottles, which allow for the performance of an appropriate number of both positive and negative tests. This is a good idea for another experiment, which could be the subject of a separate and extensive article.

The compositions of all the artificial media (substrates) used, including their $\delta^{13}C$ values, are presented in Table 1. A more detailed description of all the experimental setup procedures was presented previously [38].

Table 1. Composition of culture media, including $\delta^{13}C$ isotopic signatures of carbon sources, and experimental design for bioreactors with different dominant organic substrates (lactate, butyrate, propionate, and acetate).

Bioreactor	M1 Lactate Domination		M2 Butyrate Domination		M3 Propionate Domination		M4 Acetate Domination		
Experiment	**1**	**2**	**1**	**2**	**1**	**2**	**1**	**2**	
Media were the mixture of mineral salts [g/L]: 1.70 N_2HPO_4; 0.75 KH_2PO_4; 0.13 NaCl; 0.25 NH_4Cl; 0.5 yeast extract, supplemented with organic acid salts *:									$\delta^{13}C$ [‰]
Sodium lactate [g/L]	10.71	15.30	1.30	-	1.30	-	1.30	-	−23.0
Sodium butyrate [g/L]	1.30	-	9.00	12.80	-	-	-	-	−26.3
Sodium propionate [g/L]	-	-	-	-	9.00	12.80	-	-	−31.8
Sodium acetate trihydrate [g/L]	-	-	-	-	-	-	9.80	17.00	−45.4
Butyric acid [g/L]	-	-	-	-	0.94	-	0.94	-	−12.5
Propionic acid [g/L]	0.96	-	0.96	-	-	-	0.96	-	−31.5
Acetic acid [g/L]	0.96	-	0.96	-	1.00	-	-	-	−42.2

* Sodium lactate and acetic acid came from VWR Chemicals (Gliwice, Poland); sodium butyrate and sodium propionate from Alfa Aesar (Hesham, UK); sodium acetate from Chempur (Piekary Śląskie, Poland); butyric acid and propionic acid from Sigma Aldrich (Poznań, Poland).

Sampling for isotopic analyses was carried out during Experiment 1 at days 701–751 and in Experiment 2 at days 799–876 of bioreactor operation [38]. It is important to note that both of these periods were preceded by instances in which the medium flow was switched off in order to minimise the concentration of organic components with an unknown ^{13}C-isotope value. Furthermore, the chemical oxygen demand (COD) of the effluent from bioreactors was required to drop below 100 mg O_2/L.

2.2. Analytical Methods

The following parametres were measured: the pH of the media and the effluents from the UASB bioreactors, the redox potential (pH-meter ELMETRON model CP-502 equipped with a Combination ORP/redox, mV/electrode type ERPt-13, ELMETRON, Zabrze, Poland), the chemical oxygen demand (COD) of the medium and the effluents (NANOCOLOR COD 1500 kit, Macherey-Nagel, Düren, Germany according to ISO 15705:2002 [39]), the total biogas production rate (MGC-1 MilliGascounter, RITTER, Bochum, Germany), the composition of the biogas (HPR20 mass spectrometer, Hiden Analytical, Warrington, UK, with QGA version 1.37), and short-chain fatty acids concentrations (HPLC with photometric detection, Waters HPLC system with Waters 2996, Waters Corp., Milford, MA, USA). The apparatus utilised for this study included a Ray Detector and a 300 × 7.8 mm Aminex HPX-87 H (Bio-Rad, Hercules, CA, USA) column with a guard column, operating at a temperature of 30 °C.

Biogas samples were collected from the UASB bioreactors using a gas-tight syringe with valve and injected into 20 mL glass ampoules (tightly crimped with Teflon septa and alumina caps) filled with a supersaturated NaCl water solution. Analyses of the stable carbon isotope composition of CH_4 and CO_2 were carried out with an online method on a Delta V Advantage Mass Spectrometer coupled with a Trace GC Ultra gas chromatograph with a GC Isolink device (Thermo Fisher Scientific, Bremen, Germany). The gas chromatograph column utilised for the analysis of gases was an HP-PLOT/Q (Agilent Technologies, Folsom, CA, USA, dimensions: 30 m x 0.32 mm x 20 µm). The carrier gas was helium (purity 5.0). The GC oven was initially held at 30 °C for 4 min, and then heated at a rate of 10 °C/min to 210 °C, and held for a further 4 min. The calibration was conducted

using a CO_2-certified gas standard ($\delta^{13}C_{V\text{-}PDB} = -36.2‰$, Air Liquide GmbH, Düsseldorf, Germany). In order to ensure the accuracy of the results, the working standard CO_2 was analysed regularly using well-calibrated equipment in comparison to the $\delta^{13}C_{V\text{-}PDB}$. This process enabled the control of drift in sensitivity and the accuracy of the isotopic analysis.

The $\delta^{13}C$ analysis of the substrates was performed using a Thermo Finnigan Elemental Analyzer interfaced via a Conflow IV to a Finnigan Delta V Advantage (EA-CF-IRMS, Thermo Fisher Scientific, Bremen, Germany). A quantity of 400 µg of the sample was weighed and placed into a tin capsule, which was then sealed and packed using a hand-press device. The EA operated with an oxidation furnace temperature of 1020 °C, a reduction furnace temperature of 650 °C, and a packed-column temperature of 45 °C. In order to calibrate and normalise the ^{13}C-isotope values to the V-PDB standard, the following certified International Atomic Energy Agency (IAEA) standards were utilised: NBS-22 ($\delta^{13}C_{V\text{-}PDB} = -30.03‰$), USGS-24 ($\delta^{13}C_{V\text{-}PDB} = -16.05‰$), and USGS-40 ($\delta^{13}C_{V\text{-}PDB} = -26.39‰$). The values were recalculated and reported with reference to the Vienna Pee Dee Belemnite (V-PDB) scale, with a precision of ±0.2‰ [40,41].

Propagation error obtained using the classical derivative method for the calculated coefficient factor $\alpha^{13}C_{CO2\text{-}CH4}$ was equal to 0.0003, with significant differences at the fifth-sixth decimal place. Therefore, propagation error for the $\alpha^{13}C_{CO2\text{-}CH4}$ coefficient factor was an order of magnitude smaller than the uncertainty itself and has no practical interpretative significance.

The composition of the fermentation gas from Experiment 1 was analysed using a HPR20 mass spectrometer (Hiden Analytical, Warrington, UK) with a QGA version 1.37 and a Fisons Gas Chromatograph 8000 (Fison Instruments Ltd., Glasgow, UK) series equipped with a thermal conductivity detector.

Gas chromatography analyses were carried out for the biogas samples from Experiment 2 using a Fisons GC 8000 series. The samples were injected into a molecular sieve 5-Å column at a temperature of 40 °C; the temperature of the injector was 60 °C. The accuracy of the measurements was ±1% of gas concentration. Helium (purity 5.0) was used as carrier gas.

The statistical testing was performed using XLStat software version 2020.5.1. The calculated values were Pearson's correlation coefficient (PC), coefficient of determination (CD), and coefficient of determination in % (CD%). Values of *p*-value below 0.05 were statistically significant. The data sets used for calculation were multimodal—four separate populations, each with two experiments—for a total of eight populations (M1: 6 and 8 data sets, M2: 6 and 9 data sets, M3: 6 and 8 data sets, and M4: 5 and 8 data sets). Therefore, the number of data sets is too small to statistically significantly demonstrate normality. However, data analysed as sets separately do not show any premises to reject their normality and are consistent with a normal distribution within the limits of the experimental data.

3. Results

Bioreactor operation and biogas production summaries are presented in Table 2 [38]. Significant variation in organic acid concentrations in the effluents over time was observed in all the experimental variants (Figure 1). The highest concentrations of lactate, acetic and propionic acids were present in the effluent of bioreactor M1. The concentration of propionic acid ranged from 7.1 to 18.3 mmol/L. Acetic acid concentrations varied from 0.4 to 29.6 mmol/L. In bioreactor M2, with the domination of butyrate, the concentrations of butyric acid in the effluent ranged from 0.1 to 18.5 mmol/L. Acetic acid was present in the effluent in significantly higher concentrations as compared to other experiments (M1, M3, and M4), and varied between 10.5 and 116.1 mmol/L. Propionic acid dominated bioreactor

M3 effluent (10.8 to 42.9 mmol/L) and was supplemented by some minor concentrations of acetic acid (11.7 to 46.3 mmol/L. In the effluent of bioreactor M4, acetic acid was the main component present in the effluent, and its concentration ranged from 14.7 to 45.8 mmol/L.

Table 2. Average parameters characterising bioreactor operation during the processing of lactate-, butyrate-, propionate- and acetate-rich media.

Parameter/Bioreactor	COD [g/L]		Substrate Utilisation [%]	pH		CH_4 Content in Biogas [%]	CH_4 Production [dm^3/Day]
	Medium	Effluent		Medium	Effluent		
Experiment 1							
M1 (lactate domination)	14.1	3.7 ± 0.7	73.8 ± 5.0	5.00	7.1 ± 0.1	74.6 ± 3.0	2.3 ± 0.7
M2 (butyrate domination)	16.3	5.4 ± 0.5	66.9 ± 3.0	5.40	7.0 ± 0.7	81.5 ± 1.4	3.3 ± 0.3
M3 (propionate domination)	16.6	5.0 ± 0.5	69.7 ± 2.9	5.50	7.2 ± 0.1	81.3 ± 3.9	2.3 ± 0.5
M4 (acetate domination)	11.0	2.7 ± 0.5	75.6 ± 4.2	5.60	7.2 ± 0.1	76.2 ± 4.4	1.9 ± 0.1
Experiment 2							
M1 (only lactate)	12.2	2.2 ± 0.8	81.6 ± 6.7	7.00	7.6 ± 0.1	73.9 ± 3.8	2.6 ± 0.6
M2 (only butyrate)	16.7	5.6 ± 1.9	66.5 ± 12.9	7.10	7.2 ± 0.4	79.2 ± 2.3	2.5 ± 0.5
M3 (only propionate)	14.9	4.4 ± 1.2	70.4 ± 8.2	7.00	7.6 ± 0.1	83.8 ± 2.0	2.2 ± 0.4
M4 (only acetate)	9.5	1.8 ± 0.7	81.1 ± 7.4	7.20	7.9 ± 0.2	92.4 ± 1.3	1.4 ± 0.3

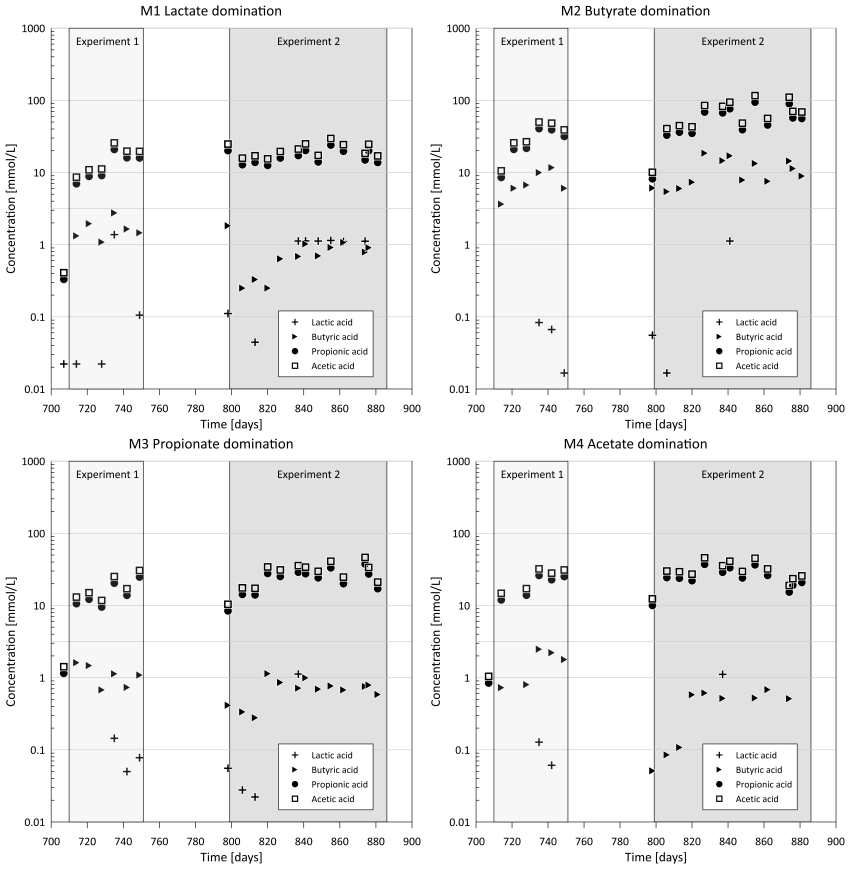


Figure 1. Variation in organic acid concentrations in the effluents from bioreactors over time during Experiments 1 and 2.

The $\delta^{13}C(CH_4)$ value of the biogas from the bioreactors varied from −58.6 to −34.8‰, while the $\delta^{13}C(CO_2)$ value ranged from −34.2 to 9.6‰, and the $\delta^{13}C(DIC)$ value ranged from −28.9 to 17.2‰ (Figure 2). The highest mean $\delta^{13}C(CH_4)$ = −36.3‰ was observed during Experiment 2, where lactate (M1) was the predominant substrate. The lowest

mean $\delta^{13}C(CH_4) = -58.1‰$ was detected in Experiment 2, where acetate (M4) was the only substrate present. The lowest mean $\delta^{13}C(CO_2)$ value (−33.4‰) was observed in Experiment 2 in the acetate substrates (M4), whereas the highest mean $\delta^{13}C(CO_2)$ value (7.2‰) occurred during Experiment 2 in the butyrate substrates (M2). The lowest mean $\delta^{13}C(DIC)$ values, −27.9‰, were observed in Experiment 2 in the acetate substrates (M4). The highest mean $\delta^{13}C(DIC)$ value, 7.2‰, was observed in Experiment 2 in the butyrate substrates (M2). The $\alpha^{13}C_{CO2\text{-}CH4}$ fractionation factor was in the range of 1.026 to 1.059 (Figure 3; Appendix B).

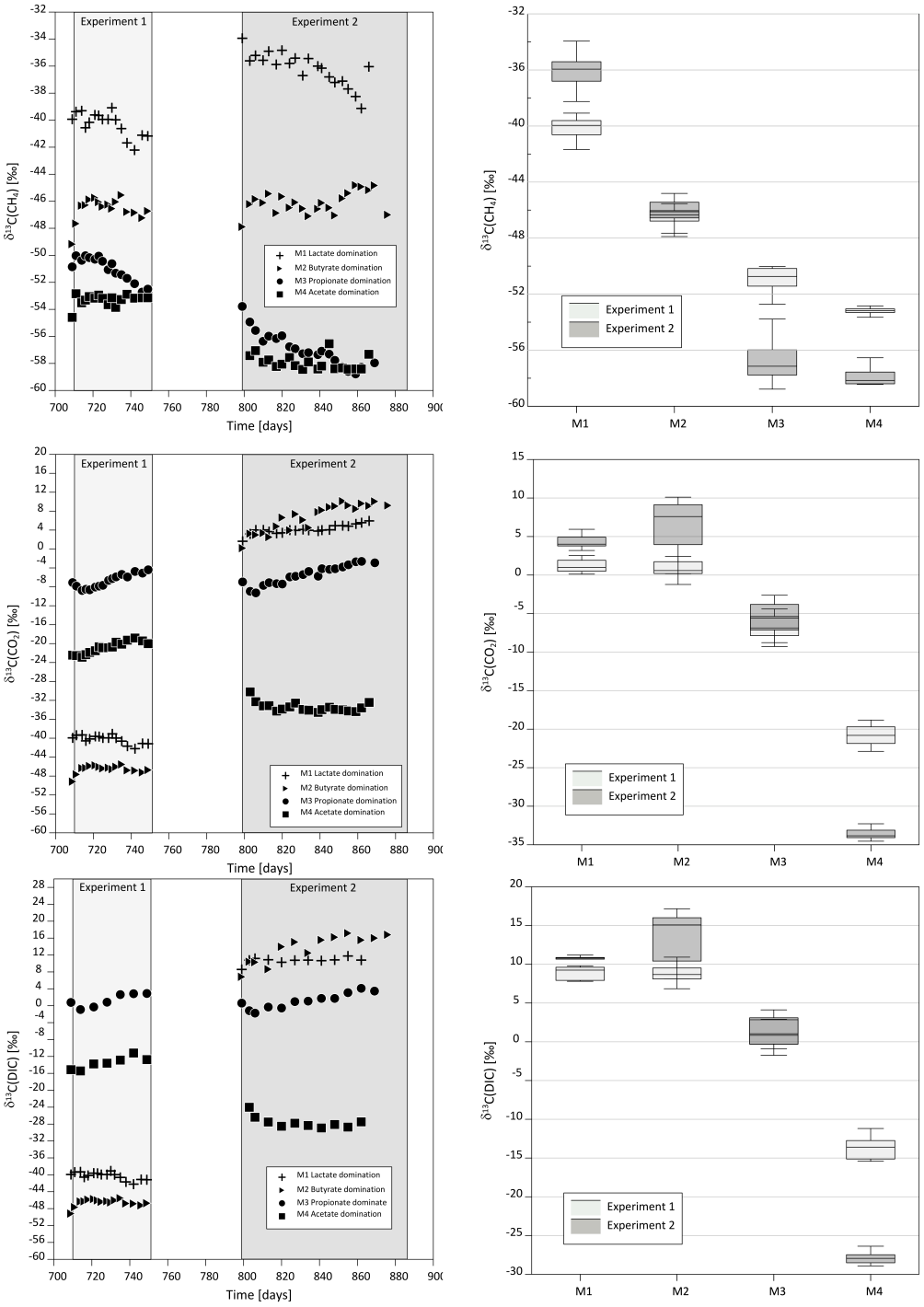


Figure 2. Variation in the $\delta^{13}C(CH_4)$, $\delta^{13}C(CO_2)$ values in the biogas and $\delta^{13}C(DIC)$ value in the effluents from bioreactors over time during Experiment 1 and Experiment 2 (mean value—centre line; minimal value—lower edge; maximal—upper edge; whiskers—range of the standard deviation).

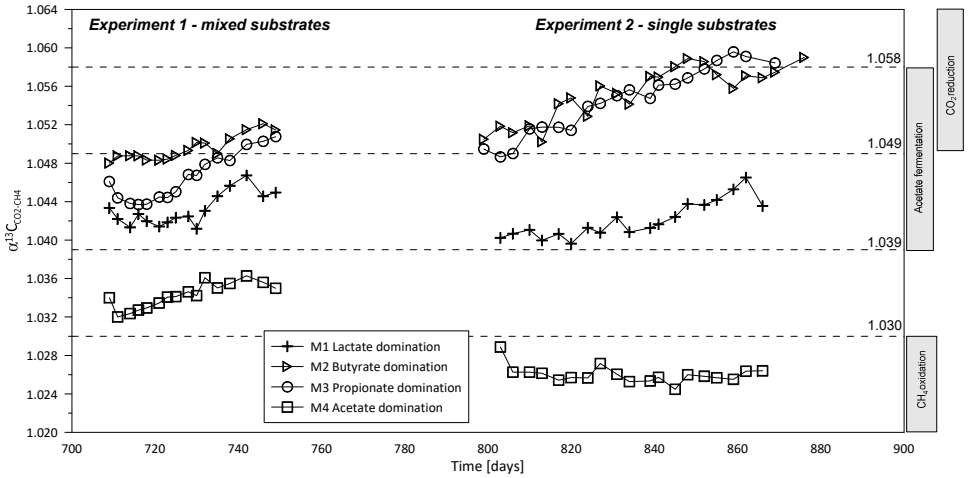


Figure 3. Variation over time of isotopic fractionation factor $\alpha^{13}C_{CO2\text{-}CH4}$ in Experiment 1 and Experiment 2.

The variation in $\delta^{13}C(CH_4)$ and $\delta^{13}C(CO_2)$ over time, as well as CH_4 yield and CO_2, are presented in Figures A1–A8 in Appendix A. The correlation of $\delta^{13}C(CH_4)$ values with CH_4 yield and $\delta^{13}C(CO_2)$ with CO_2 yield was not observed (Figures A9–A12 in Appendix A). The table with data on organic acid concentrations, biogas, and CH_4 production, as well as calculated CH_4 and CO_2 yields, are presented in Appendix B. The pH of the effluent was measured in all the bioreactors and ranged from 7.1 to 7.9. The variation in the pH values and biogas production rate (dm^3/day) is presented elsewhere [38]. The relation between the pH of the effluent and biogas production variations over time was also not observed.

To quantify the effect of organic acids on DIC formation, isotopic analysis of the DIC ($\delta^{13}C(DIC)$) and $\alpha^{13}C_{CO2\text{-}CH4}$ statistical tests were carried out. In Experiment 1, both the $\delta^{13}C(DIC)$ and $\alpha^{13}C_{CO2\text{-}CH4}$ values showed noticeable correlations with lactic and butyric acid concentrations, which explain 19% of the variance in DIC and 23% of the variance in $\alpha^{13}C_{CO2\text{-}CH4}$. In Experiment 2 the $\delta^{13}C(DIC)$ values are correlated with butyric acid concentration, especially when compared to Experiment 1 (Table 3). The values of $\alpha^{13}C_{CO2\text{-}CH4}$ correlate most strongly with lactic acid (CD: 28%), followed by propionic acid (CD: 16%), and acetic acid (CD: 13%).

Table 3. The statistical tests of correlation between concentrations of dominated organic acids in effluents from bioreactors, $\delta^{13}C(DIC)$ and fractionation factor $\alpha^{13}C_{CO2\text{-}CH4}$ in biogas from Experiment 1 and Experiment 2.

Product	Statistics	M1 lactate domination	M2 butyrate domination	M3 propionate domination	M4 acetate domination
$\delta^{13}C(DIC)$	PC	*0.27*	*0.49*	0.17	0.18
	p	*0.05*	*0.00*	0.20	0.18
	CD	*0.07*	*0.24*	0.03	0.03
	CD%	7	24	3	3
$\alpha^{13}C_{CO2\text{-}CH4}$	PC	0.05	*0.52*	*0.40*	*0.34*
	p	0.69	*0.00*	*0.00*	*0.01*
	CD	0.00	*0.27*	*0.16*	*0.12*
	CD%	0	27	16	12

Table 3. *Cont.*

Product	Statistics	M1 lactate domination	M2 butyrate domination	M3 propionate domination	M4 acetate domination
Experiment 1					
Product	Statistics	M1	M2	M3	M4
$\delta^{13}C(DIC)$	PC	0.175	*0.44*	0.17	0.09
	p	0.424	*0.04*	0.44	0.67
	CD	0.03	*0.19*	0.03	0.01
	CD%	3	19	3	1
$\alpha^{13}C_{CO2-CH4}$	PC	0.030	*0.48*	0.36	0.29
	p	0.892	*0.02*	0.09	0.18
	CD	0.00	*0.23*	0.13	0.08
	CD%	0	23	13	8
Experiment 2					
Product	Statistics	M1	M2	M3	M4
$\delta^{13}C(DIC)$	PC	0.305	*0.51*	0.18	0.25
	p	0.085	*0.00*	0.30	0.16
	CD	0.093	*0.26*	0.03	0.06
	CD%	9	26	3	6
$\alpha^{13}C_{CO2-CH4}$	PC	0.057	*0.53*	*0.40*	*0.36*
	p	0.754	*0.00*	*0.02*	*0.04*
	CD	0.003	*0.28*	*0.16*	*0.13*
	CD%	0.03	28	16	13

PC—Pearson's coefficient. *p*—statistical significance. CD—coefficient of determination. CD%—coefficient of determination in %. Italics—parameters statistically significant with *p*-value < 0.05.

When comparing the results from Experiments 1 and 2, one may infer that the lactic and butyric acids contributed most to new portions of DIC because they exerted most influence on the $\delta^{13}C(DIC)$ value, and the CD [%] ranged up to 24% (Table 3). Overall, the CD values were low to moderate, indicating that the tested models explained up to 28% of the observed variability. Although the explanatory power was limited, such values can still be considered meaningful in biological and environmental studies, where multiple interacting factors often influence the investigated processes.

4. Discussion

This study advances the work [38] which focused mostly on bioreactors' performance and metagenomics to identify acidogenesis products on the course of acetogenesis and methanogenesis as well as the microbial community dynamics. We used isotopic tracing of these processes with a focus on isotopic fractionation and quantitative assessment of methanogenic pathways. We employed comparative analysis to construct a detailed picture of the distribution of carbon molecules from the substrates to the products while paying special attention to sources of CH_4 formation. Concentrations of organic acids were monitored in the effluents and headspace gas samples and effluents were collected for geochemical and stable isotope analyses. Non-labelled compounds that differed in the $\delta^{13}C$ value of bulk organic matter were used as substrates.

The chemical oxygen demand (COD) in the bioreactor effluents significantly decreased in time throughout Experiments M1, M2, M3, and M4, compared with the supplied substrates in media (Figure 4). The rate of COD decrease was the highest in Experiment 1 in the acetate-dominant substrates (M4, 75%) and in Experiment 2 with the domination of lactate (M1, 82%). The lowest COD reduction was observed during butyrate degradation (67 and 63% in Experiment 1 and Experiment 2, respectively). These results indicate that lactate and acetate were preferentially decomposed at a higher rate. Butyrate was the most resistant compound for oxidation.

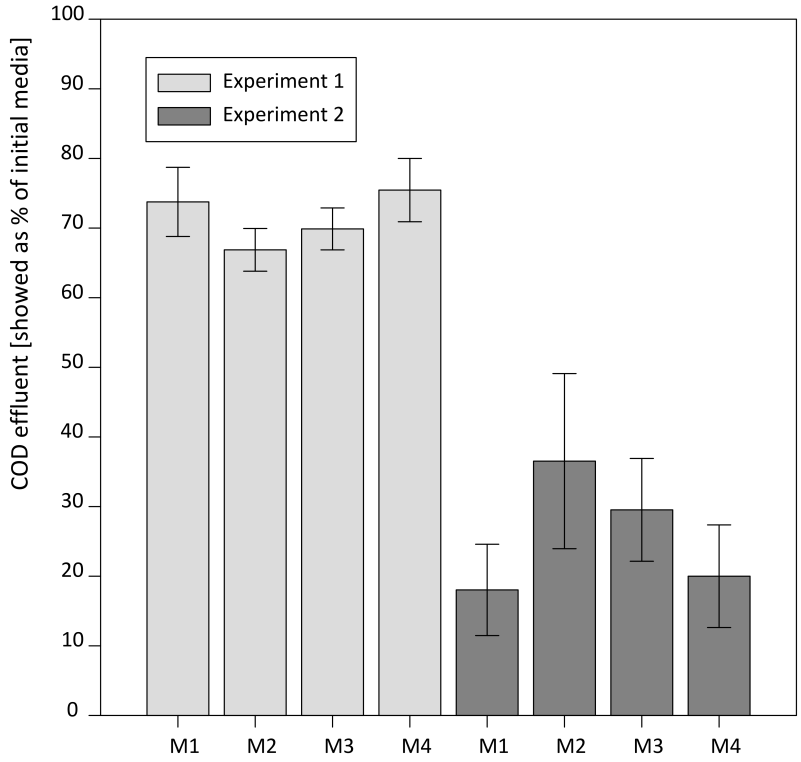


Figure 4. The chemical oxygen demand (COD) reduction during Experiments 1 and 2.

The concentration of the individual media components significantly changed over time in all experiments. The measurements of their concentrations in the effluents helped to determine the biogeochemical reactions during the processes. Lactic, butyric, and propionic acid were decomposed to acetic acid—the direct precursor of methanogenesis. Lactic acid was also almost completely utilised in all bioreactors independent of its initial concentration in the media, suggesting that lactate is the most energetically attractive substrate for acetogenic bacteria [42]. This may also be explained by an unknown symbiotic microbial consortium that acts selectively in advance of lactate or components outside the scope of these experiments. Propionic acid was present in the effluent from bioreactors containing lactate, butyrate, and acetate-rich media. It may reflect contributions of other metabolic pathways in bioreactors, e.g., lactate processing to propionate or amino acids degradation [35]. Acetic acid was present in all bioreactors, which resulted in the formation of CH_4 via the acetate decarboxylation pathway.

The $\delta^{13}C(CH_4)$ values obtained in biogas from bioreactors varied within the range from −57.2 to −36.2‰. Such elevated $\delta^{13}C$ values are typical for CH_4 formed exclusively or in the majority from acetate decarboxylation [7,18,19]. In both experiments, M1 (Experiment 1) with a lactate-dominant mixture of organic acid salts, and M2 (Experiment 2) with a single lactate compound, we observed similar isotopic fractionation of carbon isotopes between CH_4 and CO_2, $\alpha^{13}C_{CO2\text{-}CH4}$ equal 1.043 and 1.042, respectively. This difference, in practice,

is comparatively negligible when combined with experimental and analytical errors. In experiments with the butyrate-rich (M2) and propionate-rich (M3) media, we observed enrichment of the CH_4 in light carbon isotopes, which can be attributed to CO_2 reduction. This observation is confirmed by a concurrent increase in the isotopic fractionation factor $\alpha^{13}C_{CO2\text{-}CH4}$ (Figure 3) [38].

In Experiments 1 and 2 with acetate (M4) as the dominant substrate, the $\delta^{13}C(CH_4)$ value comprised a very narrow range from −53.3 to −57.2‰, respectively. Such $\delta^{13}C(CH_4)$ values are within the lowermost range of $^{13}C/^{12}C$ in CH_4 formed due to the acetate decarboxylation pathway. During the continuous loading anaerobic digestion conducted for 170 days [32], $\delta^{13}C(CH_4)$ values also showed a quite large range between −60‰ and −40‰, with a step increase from 54‰ to 40‰ at the end of the experiment. Short-term fluctuations in the values of $\delta^{13}C(CH_4)$, ranging from 2.5 to 5.0‰, are explained by feeding events when loading the bioreactor.

The $\delta^{13}C(CO_2)$ values from the acetate-dominated incubations (M4) in Experiments 1 and 2 were −20.9 and −33.4‰, respectively. This is beyond any question that the difference between isotopic ratios $\delta^{13}C(CO_2)$ = 12.5‰ is significant. The corresponding $\delta^{13}C(CH_4)$ values in these two experiments amounted to −53.3 and −57.9, respectively, causing an isotopic difference in $\delta^{13}C(CH_4)$ = 4.6‰. Isotopic fractionation factors $\alpha^{13}C_{CO2\text{-}CH4}$ were therefore equal to 1.034 and 1.026, respectively (Figure 3; Appendix B). The $\alpha^{13}C_{CO2\text{-}CH4}$ results reported here are close to acetate decarboxylation and/or can be considered as typical for CH_4 oxidation resulting in ^{13}C enrichment of the residual CH_4 [8,18,29,43–45]. The possibility of CH_4 oxidation was generally excluded because free oxygen was absent in headspace and in the liquids, and the process was anaerobic (redox potential in the range from −400 to −255 mVal). Sulphates or nitrates were not present in the M9 minimal medium. However, iron and sulphur were in the effluent from bioreactors in very low concentrations ($S^{2-} \leq 0.2$ mg/L and $Fe^{2+/3+} \leq 1.5$ mg/L). This suggests that anaerobic CH_4 oxidation on a very small scale cannot be ruled out [38].

From our experiments, we infer that the high concentrations of acetate always resulted in the formation of CO_2 enriched in light carbon isotopes, when compared to the CO_2 obtained from the lactate-, butyrate-, and propionate-rich experiments. Our experiments were carried out in the open system, where the fresh substrate was continuously supplemented to the bioreactor to maintain stability. Consequently, this resulted in a typical Rayleigh distillation effect. Here, ^{12}C-acetate was permanently decomposed faster than ^{13}C-acetate compared to their relative abundance in the bulk acetate particles present in the solution, yielding ^{13}C-depleted CO_2. Products of biodegradation from laboratory experiments in closed systems may be enriched in heavy carbon isotopes to values higher than the starting precursor material [18]. In such cases, when isotopic equilibration is absent, a kinetic isotope effect is expected, the main driver of which is the ^{12}C-depletion of the substrate throughout its consumption. Resupply of acetate limits this effect and better reflects natural conditions, where permanent production of new born acetate appears in the system.

In other experiments, in which a detritic lignite and xylite were microbially decomposed, the isotopic fractionation factor $\alpha^{13}C_{CO2\text{-}CH4}$ was also typical for CH_4 oxidation [46,47]. Although CH_4 oxidation can occur in many anaerobic environments and in anaerobic incubation experiments, it seems that in the case of detritic lignite and xylites it is driven by substrate depletion. Enrichment of CH_4 in ^{13}C in the case of MCBM is a result of degradation of methoxyl groups and O-demethylation reactions [48].

Geological organic materials are more resistant to microbial decomposition than any fresh biological one due to the lower content of the easiest-utilised compounds (e.g., sugars—cellulose and hemicelluloses). High-energy-profit enzymatic reactions are absent as the relevant substrates are depleted. Therefore, natural substrates like maize silage or

cattle manure are interesting materials to study CH_4 and CO_2 systems. In this context, we compared the results from Experiment 1 and Experiment 2 of our study with data from other experiments using natural substrates in closed systems [46,47,49]. Both experiments were performed in headspace gas bottles closed with rubber septa, with minimal M9 media, stored at room temperature (21–22 °C) with the addition of the methanogenic microorganisms collected from the anaerobic digestion chamber [46]. We observed that the isotopic fractionation factor $\alpha^{13}C_{CO2\text{-}CH4}$ for fresh cattle manure (FCA) and maize silage (MS) is in a similar range, from 1.038 to 1.041, whereas decomposed cattle manure is characterised by $\alpha^{13}C_{CO2\text{-}CH4}$ equal to 1.025 (Figure 5). We concluded that in the case of biological and material from incubation experiments, isotopic data should indicate CH_4 oxidation solely as a result of substrate depletion. This is important for applications of stable isotope probing in the industry and biotechnology as well as other commercial purposes.

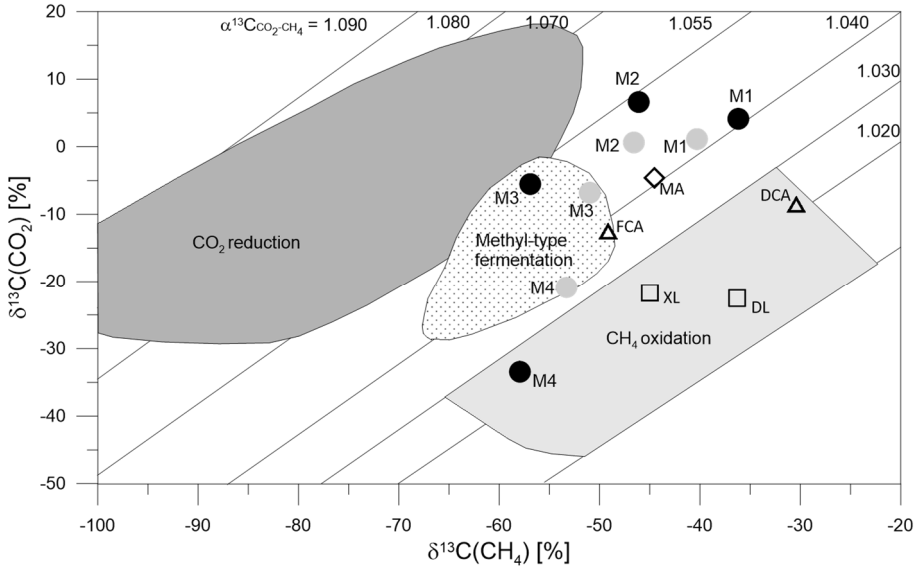


Figure 5. The mean $\delta^{13}C(CH_4)$ and mean $\delta^{13}C(CO_2)$ values in Experiments 1 and 2 and their comparison with the results from other incubation experiments (Experiment 1—grey circles; Experiment 2—black circles; DL—detritic lignite; XL—xylite; MA—maize silage; FCA—fresh cattle manure; DCA—decomposed cattle manure; MA, FCA, DCA—Refs. [46,47,49] overlayed on the discrimination graph by Whiticar [18].

Mixing of different substrates in fermentation solutions results in many difficulties in interpreting isotopic data. The results are often combined using linear regressions. For our studies, we observed that the obtained $\delta^{13}C(CO_2)$ values were strongly correlated with $\delta^{13}C(DIC)$ values (Figure 6), which indicate stable conditions during incubation and isotopic equilibrium of CO_2 with DIC.

No correlation between the calculated $\Delta^{13}C_{SUB\text{-}CH4}$, $\Delta^{13}C_{SUB\text{-}CO2}$, and $\Delta^{13}C_{SUB\text{-}DIC}$ was observed. This confirms that each substrate was decomposed at a different rate, which is expressed in the variation of the isotopic fractionation factor. A significant correlation between $\Delta^{13}C_{CO2\text{-}CH4}$ and $\Delta^{13}C_{CO2\text{-}DIC}$ was observed for Experiment 1 and Experiment 2, at 0.96 and 0.78, respectively (Figure 7). The experiments with single substrates were also characterised by higher values of $\Delta^{13}C_{CO2\text{-}DIC}$ than experiments with mixed substrates. This indicates that the decomposition of single substrates resulted in a narrower range of $\delta^{13}C(CO_2)$ and $\delta^{13}C(DIC)$, which is caused by the decomposition of only one, dominant compound. When substrates are mixed, there are more possible sources of CO_2 and DIC, which results in lower values of $\Delta^{13}C_{CO2\text{-}DIC}$.

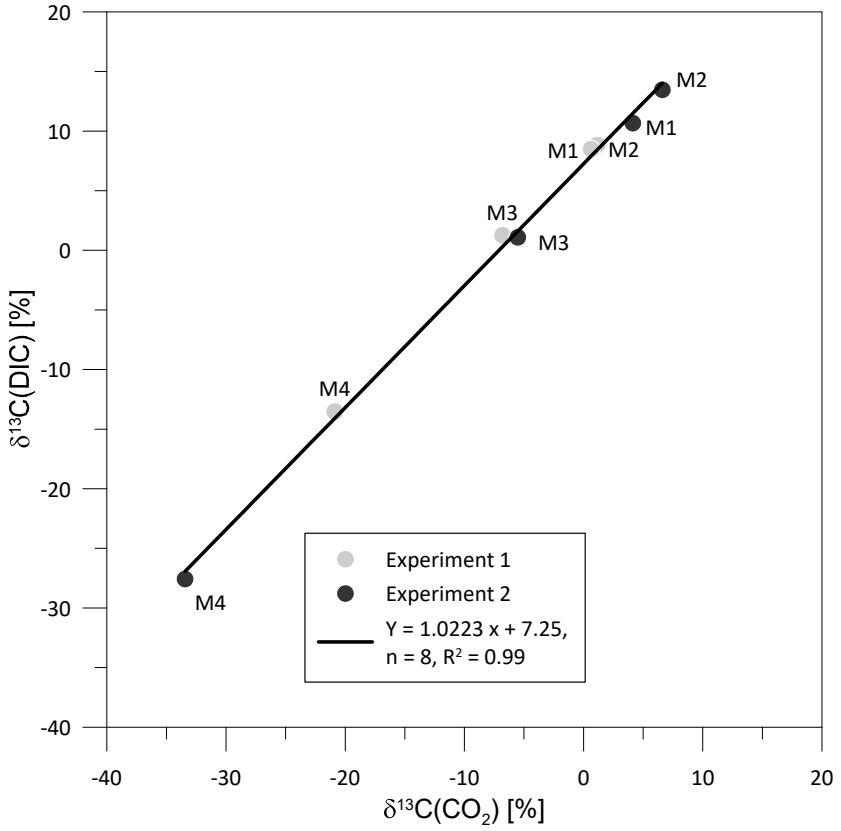


Figure 6. Correlation of the mean $\delta^{13}C(CO_2)$ and $\delta^{13}C(DIC)$ values from all incubations.

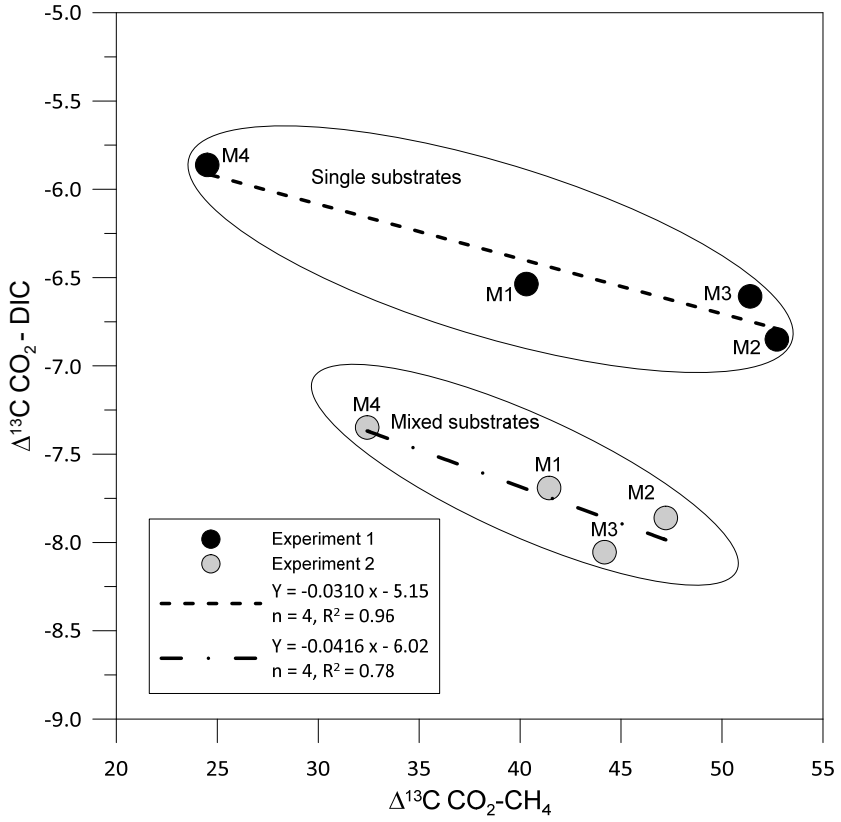


Figure 7. Correlation of the $\Delta^{13}C_{CO2\text{-}CH4}$ and $\Delta^{13}C_{CO2\text{-}DIC}$ from all incubations.

Statistical tests suggest that propionate and acetate were degraded mostly to CH_4, the product of low solubility in the effluent, and released immediately to the headspace. The

presence of butyric acid, which is the most resistant product for microbial decomposition, resulted in the enrichment of DIC and CO_2 in heavy carbon isotopes. However, isotopic mass balance calculations of substrates and products in the case of our experiments are very difficult to perform, and thus make modelling of microbial processes with the connection to the isotope picture very difficult. The microbial processes in open systems with mixed microbial communities are complex, including both heterotrophic and syntrophic reactions. The main contributors to biomethanation were likely *Methanothrix soehngenii* and *Methanoculleus* sp. Acetate appeared to be primarily utilised by *Smithellaceae* sp., potentially in competition with *M. soehngenii*. Propionate dismutation and β-oxidation pathways may have been interconnected through butyrate exchange among putative syntrophic partners, including members of the *Syntrophomonadaceae* and *Smithellaceae* families [37,38]. However, most of the methanogens in our cultures were not identified in the databases, which makes studies of microbial communities in open systems challenging. Modelling for isotope studies is usually preceded by separate degradation experiments of individual bacterial strains capable of using a specific chemical compound as an energy source under controlled, sterile conditions [50]. Such experimental series allow for the determination of an isotopic fractionation coefficient, which can then be applied to field and environmental studies. Application of ^{13}C-labelling substrates on specific positions allow to verify the specific degradation pathways and provides data which can be used for further modelling. Such models based can be used to evaluate environmental or experimental data for simple processes, such as mixing or even more complex processes based on many assumptions. One of those models is FRAME—a Monte Carlo model for evaluation of the stable isotope mixing and fractionation [51]. The multitude of biochemical reactions in cultures with mixed microbial communities is extremely challenging. The same organic compounds that are provided as a source of energy and carbon for microorganisms can be synthesised by other microorganisms, making mass balance difficult to perform. Analysis of such data will undoubtedly advance in the future (thanks to, among other things, the development of AI technology and the development of clumped isotope research). However, providing the data necessary to build a specific model still requires a significant amount of work and, above all, the identification of unknown methanogenesis pathways.

5. Conclusions

This study revealed that acidogenesis products—lactate, butyrate, propionate, and acetate—are processed to CH_4 by the acetate decarboxylation pathway. Acetate is derived from the decomposition of lactate, butyrate, and propionate. The CO_2 reduction pathway of methane synthesis was observed in experiments with butyrate and propionate as the substrates. The isotopic analyses of carbon in CH_4 and CO_2 revealed that the isotopic fractionation factor $\alpha^{13}C_{CO2\text{-}CH4}$ was typical for acetate decarboxylation in the case of experiments with lactate- and acetate-rich media. Decomposition of butyrate and propionate resulted in the formation of CH_4 by both CO_2 reduction and acetate decarboxylation pathways. The $\delta^{13}C(DIC)$ values were strictly dependent on the carbon isotopic composition of CO_2, which indicates that CO_2 from headspace gas was in equilibrium with DIC. The $\delta^{13}C(DIC)$ value was strongly influenced by butyrate, the substrate most resistant to decomposition in this study.

Comparison of mean $\delta^{13}C(CH_4)$ and $\delta^{13}C(CO_2)$ values from Experiment 1 and Experiment 2 with other experiments using natural substrates (detritic lignite, xylite, maize silage, and cattle manure) showed that the isotope fractionation factor $\alpha^{13}C_{CO2\text{-}CH4}$ differs significantly between open and closed experimental systems. Continuous delivery of fresh acetate to the bioreactor resulted in the formation of CO_2 enriched in light carbon isotopes. This shifts the isotope fractionation factor $\alpha^{13}C_{CO2\text{-}CH4}$ to values typical for CH_4 oxidation.

Microbial CH_4 is further oxidised during methanogenic decomposition in a closed system of depleted substrates such as detritic lignite, xylite, or cattle manure. Investigation of the stable carbon isotopes in open system incubations should be very carefully interpreted and account for other parameters such as organic acid concentrations. This conclusion is important for applications of stable isotope probing in the industry and biotechnology. Overall, this study underscores that integrating isotope-based insights into methanogenic processes can drive the optimisation of sustainable biotechnological systems, enhancing carbon efficiency and supporting low-emission energy production. Such knowledge is particularly relevant for advancing sustainable biogas technologies, where maximising energy recovery from organic waste while minimising environmental impact is a key priority.

Author Contributions: Conceptualisation—M.B., A.D.-I., M.O.J. and A.S.; methodology—M.B., A.C. and A.D.-I.; formal analysis—M.B., A.D.-I. and E.Ł.; investigation—B.B., A.C., A.D.-I., W.D., M.J., D.K. and Ł.P.; resources—M.O.J. and A.S.; writing—original draft—M.B., A.D.-I., M.O.J. and A.S.; writing—review and editing—M.J., E.Ł. and A.T.-O.; visualisation—M.B. and A.D.-I.; supervision—M.O.J. and A.S.; project administration—A.S.; funding acquisition—A.S. All authors have read and agreed to the published version of the manuscript.

Funding: This research was funded in part by The National Science Centre, Poland through projects 2015/17/B/NZ9/01718 (AS) and 2023/51/B/ST10/02794 (MB). Anna Detman-Ignatowska was supported by the Foundation for Polish Science (FNP). For the purpose of Open Access, the author has applied a CC-BY public copyright licence to any Author Accepted Manuscript (AAM) version arising from this submission.

Institutional Review Board Statement: Not applicable.

Informed Consent Statement: Not applicable.

Data Availability Statement: The original contributions presented in this study are included in the article. Further inquiries can be directed to the corresponding author. Raw data from metagenomic and metatranscriptomic analyses generated in this study have been deposited in the NCBI under BioProject number PRJNA972863.

Acknowledgments: We thank the three anonymous reviewers for their constructive comments and support throughout the revision process. The authors have reviewed and edited the output and take full responsibility for the content of this publication.

Conflicts of Interest: The authors declare no conflicts of interest.

Abbreviations

The following abbreviations are used in this manuscript:

CD	Coefficient of Determination
COD	Chemical Oxygen Demand
DIC	Dissolved Inorganic Carbon
MCBM	Microbial Coal Bed Methane
PC	PC—Pearson's correlation coefficient
UASB	Up-flow Anaerobic Sludge Blanket

Appendix A. Additional Plots for the Section Results

Additional variation and correlation plots for Experiments 1 and 2 (Section 3—Results).

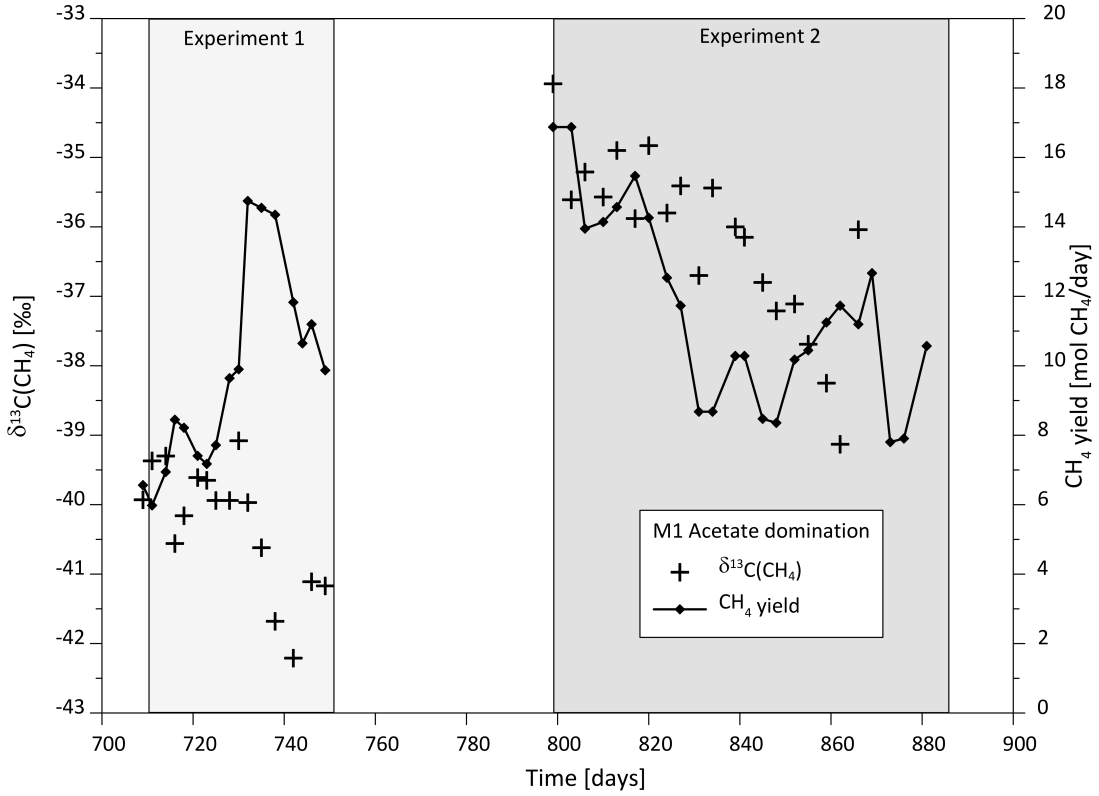


Figure A1. Variation in $\delta^{13}C(CH_4)$ and CH_4 yield over time in Experiment M1 with lactate domination.

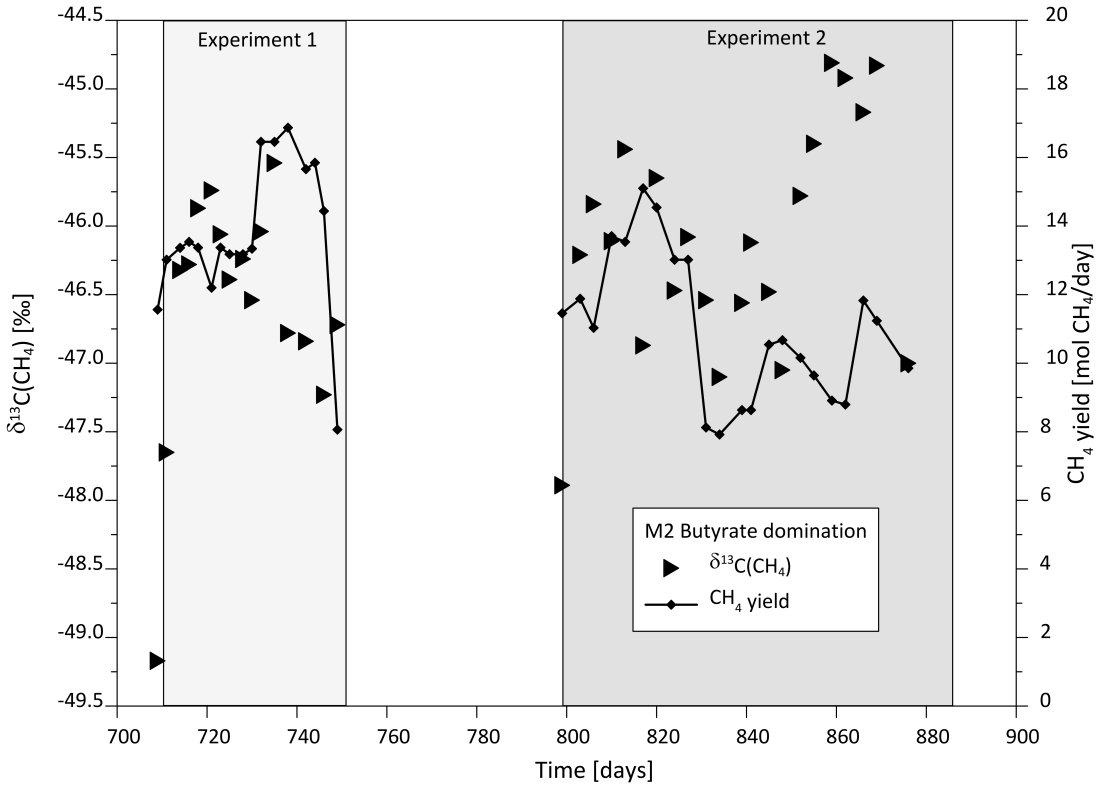


Figure A2. Variation in $\delta^{13}C(CH_4)$ and CH_4 yield over time in Experiment M2 with butyrate domination.

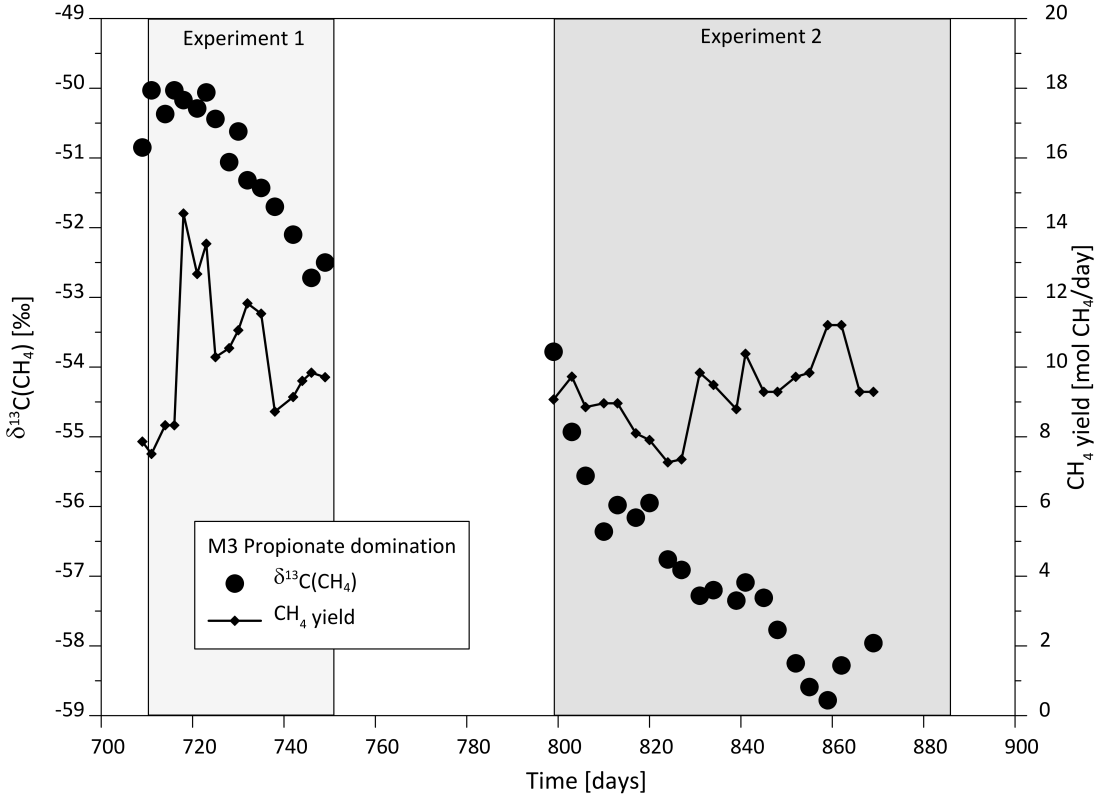


Figure A3. Variation in $\delta^{13}C(CH_4)$ and CH_4 yield over time in Experiment M3 with propionate domination.

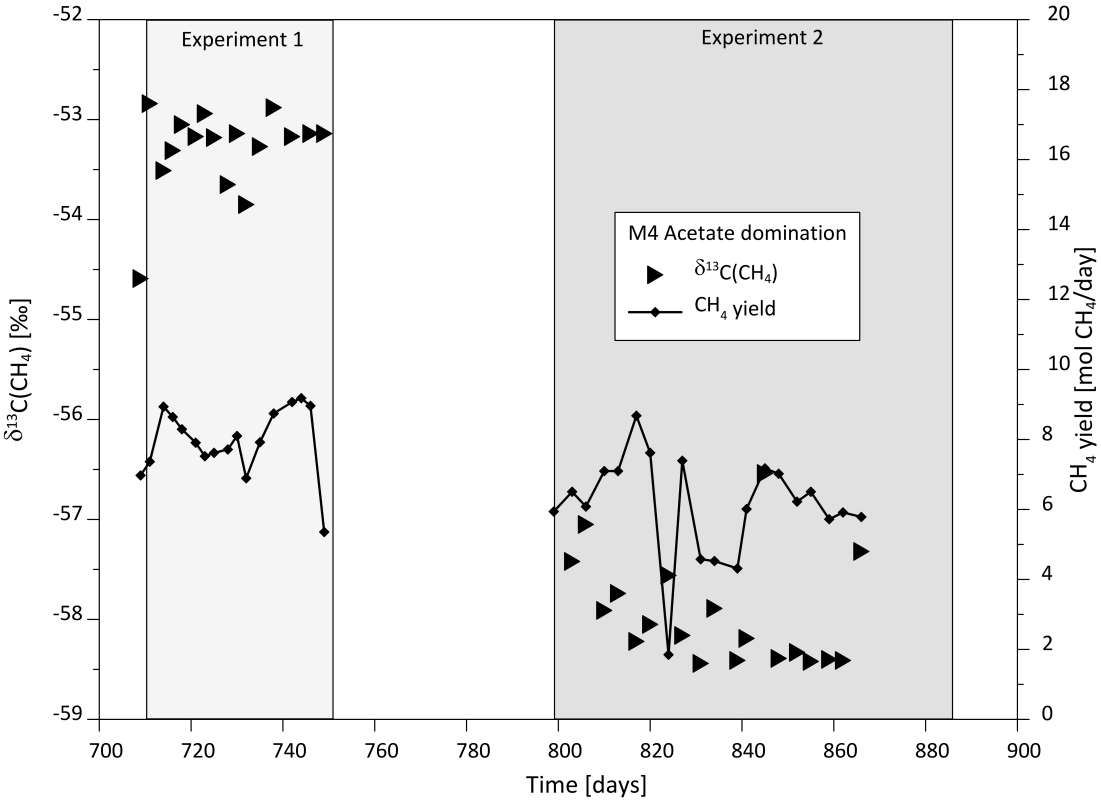


Figure A4. Variation in $\delta^{13}C(CH_4)$ and CH_4 yield over time in Experiment M4 with acetate domination.

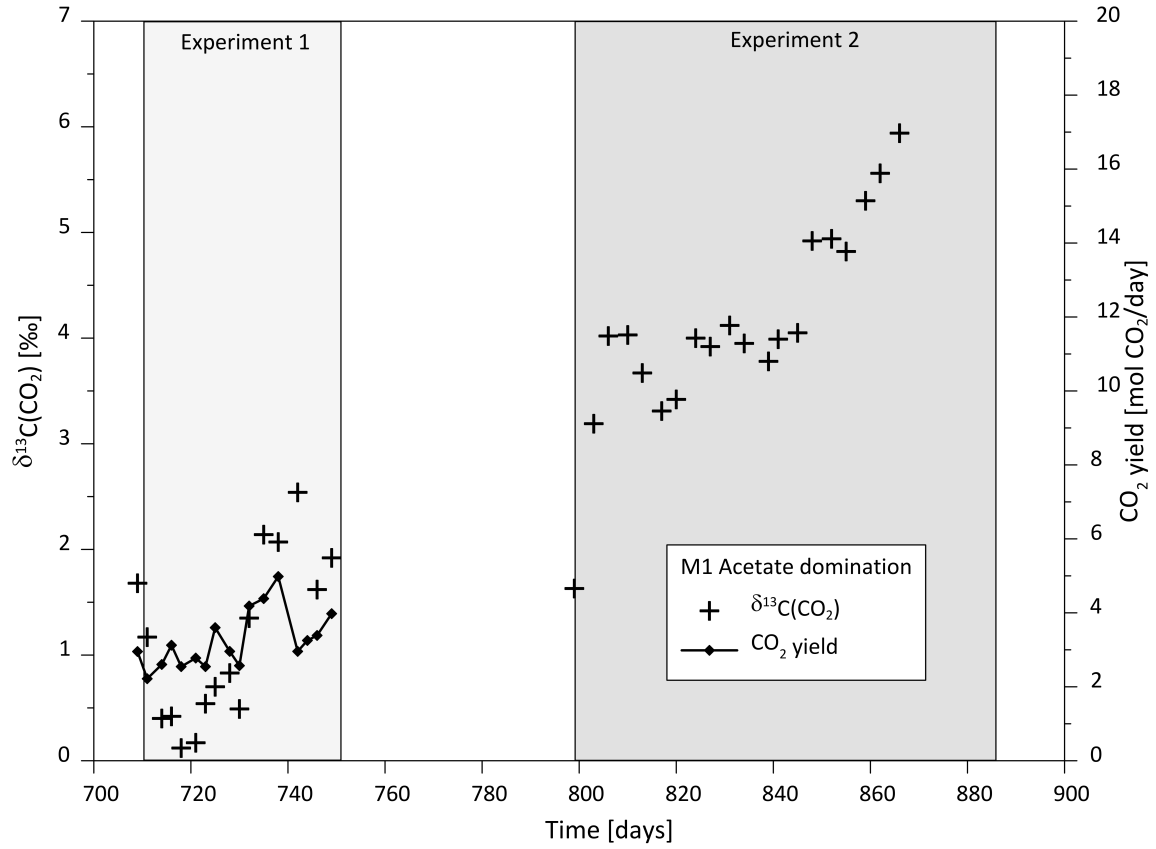


Figure A5. Variation in $\delta^{13}C(CO_2)$ and CO_2 yield over time in Experiment M1 with lactate domination.

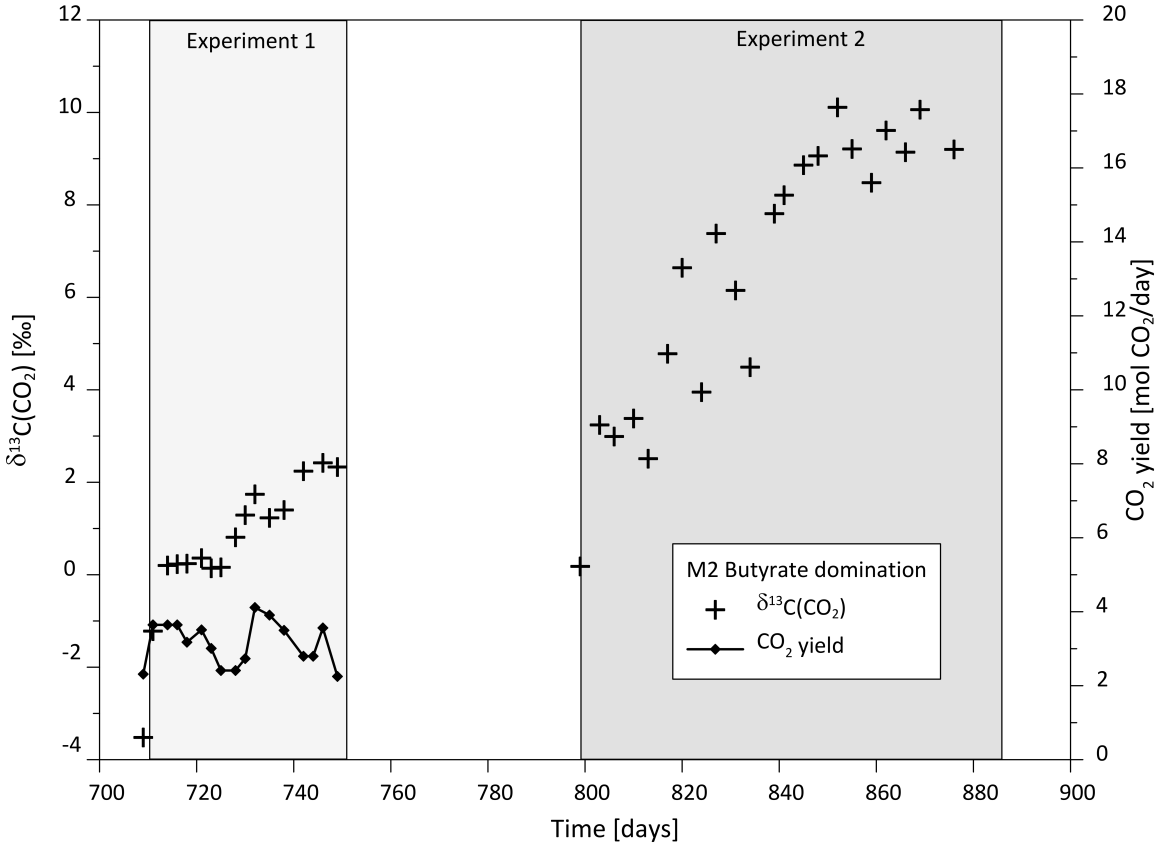


Figure A6. Variation in $\delta^{13}C(CO_2)$ and CO_2 yield over time in Experiment M2 with butyrate domination.

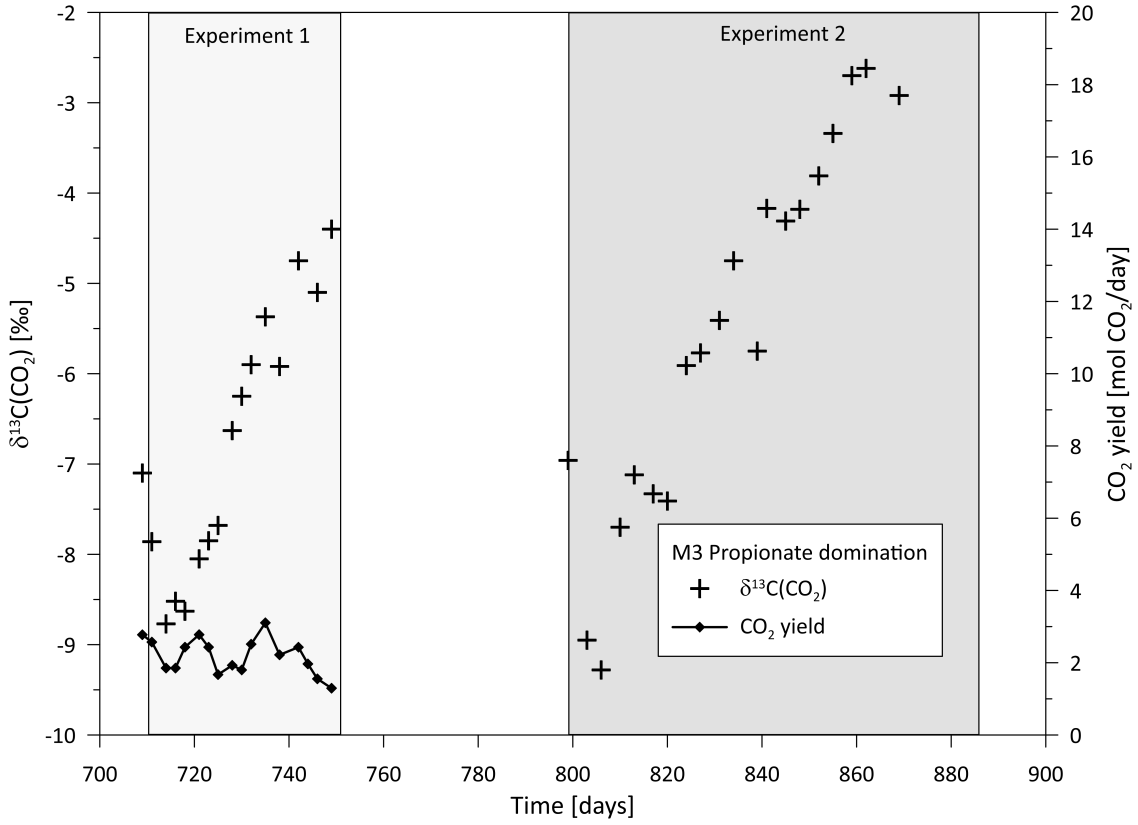


Figure A7. Variation in $\delta^{13}C(CO_2)$ and CO_2 yield over time in Experiment M3 with propionate domination.

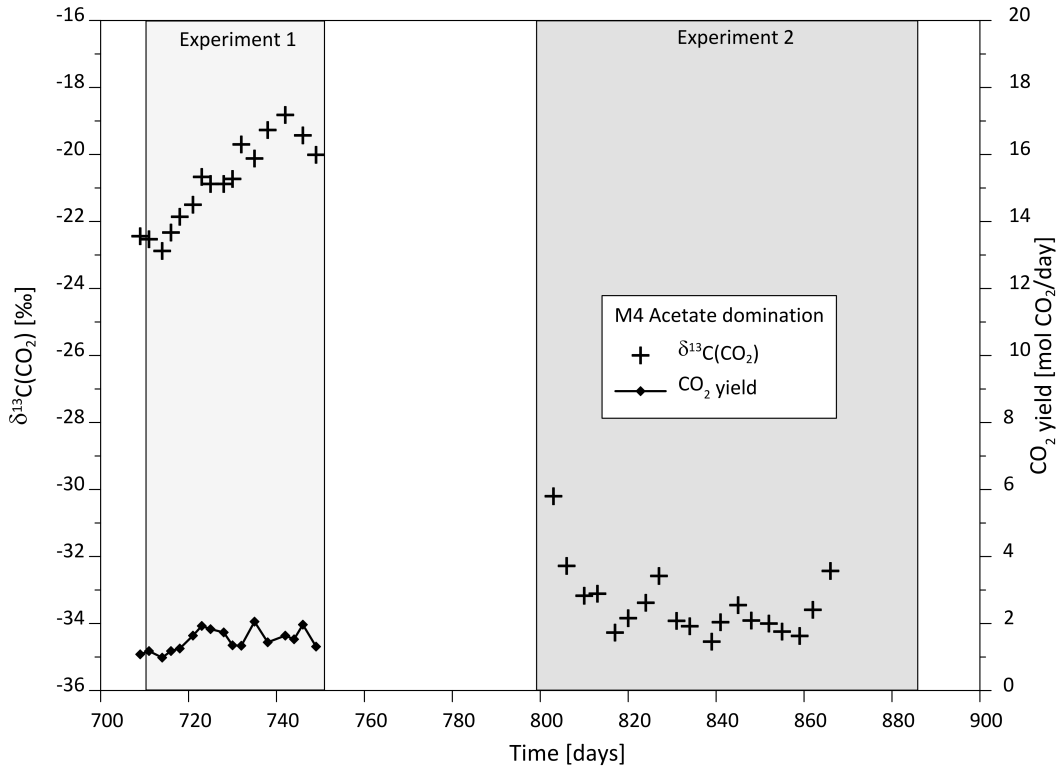


Figure A8. Variation in $\delta^{13}C(CO_2)$ and CO_2 yield over time in Experiment M4 with acetate domination.

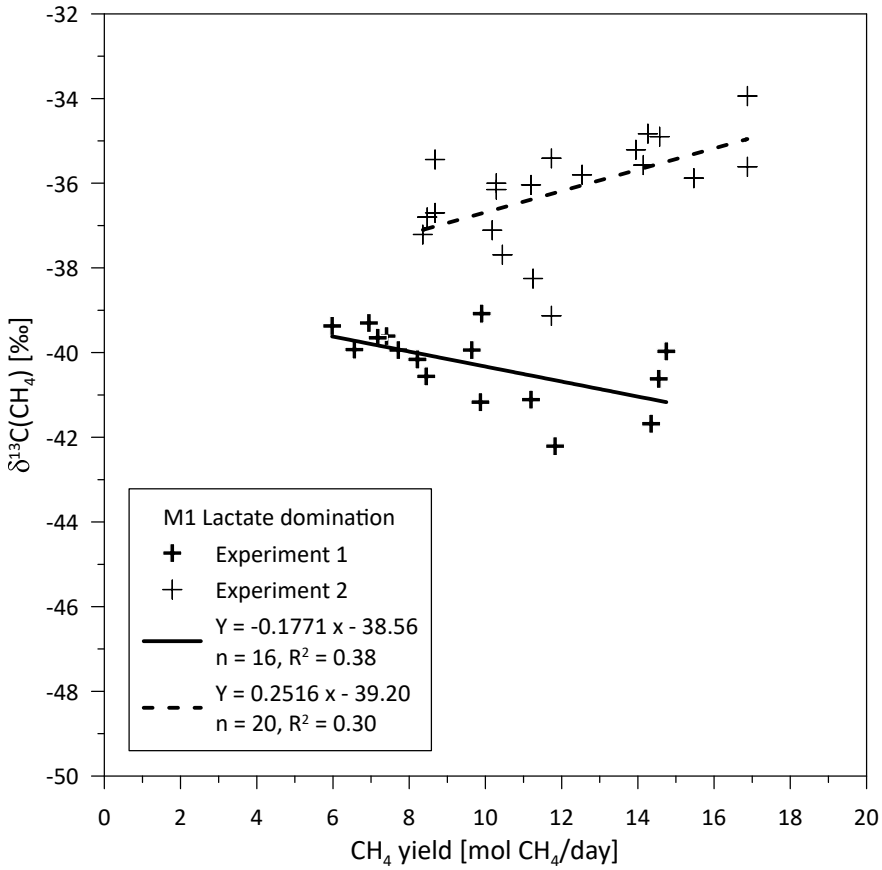


Figure A9. Correlation of $\delta^{13}C(CH_4)$ values and CH_4 yield in Experiment M1 with lactate domination.

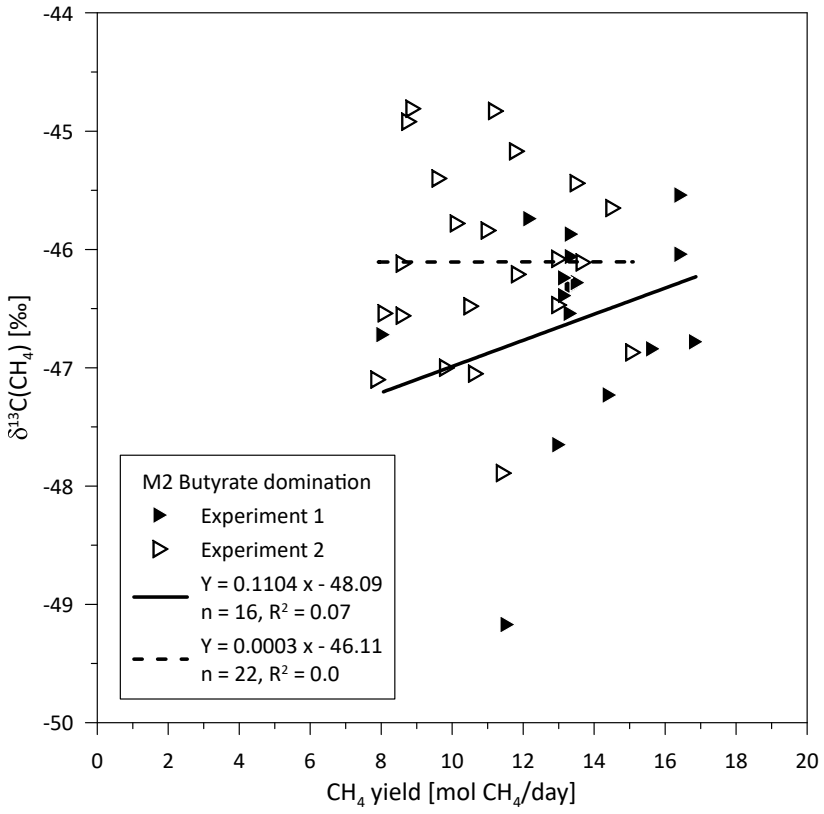


Figure A10. Correlation of $\delta^{13}C(CH_4)$ values and CH_4 yield in Experiment M2 with butyrate domination.

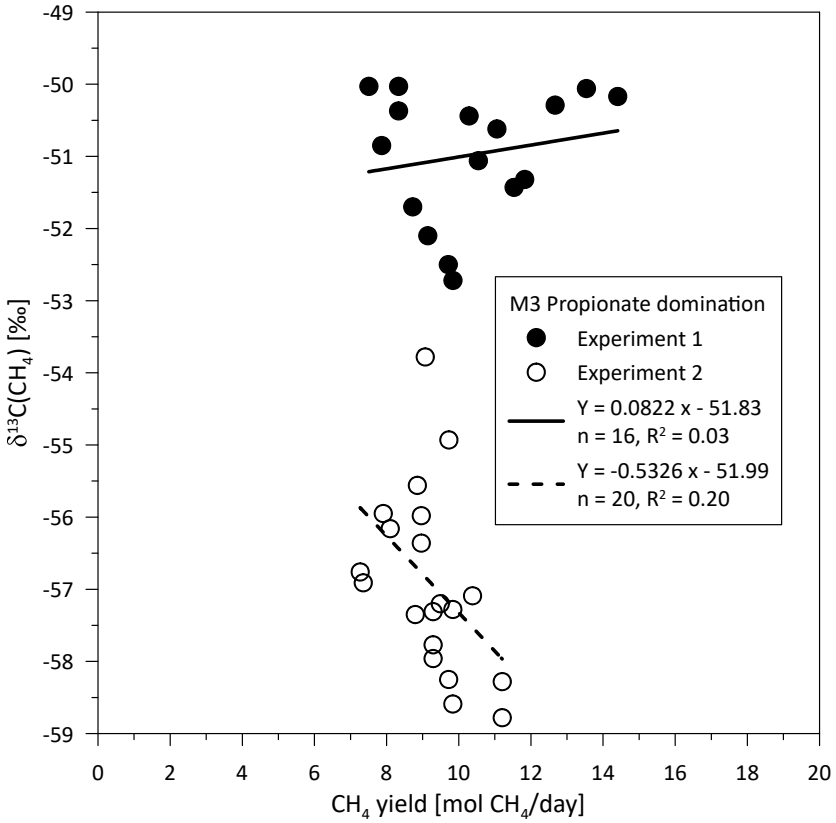


Figure A11. Correlation of $\delta^{13}C(CH_4)$ values and CH_4 yield in Experiment M3 with propionate domination.

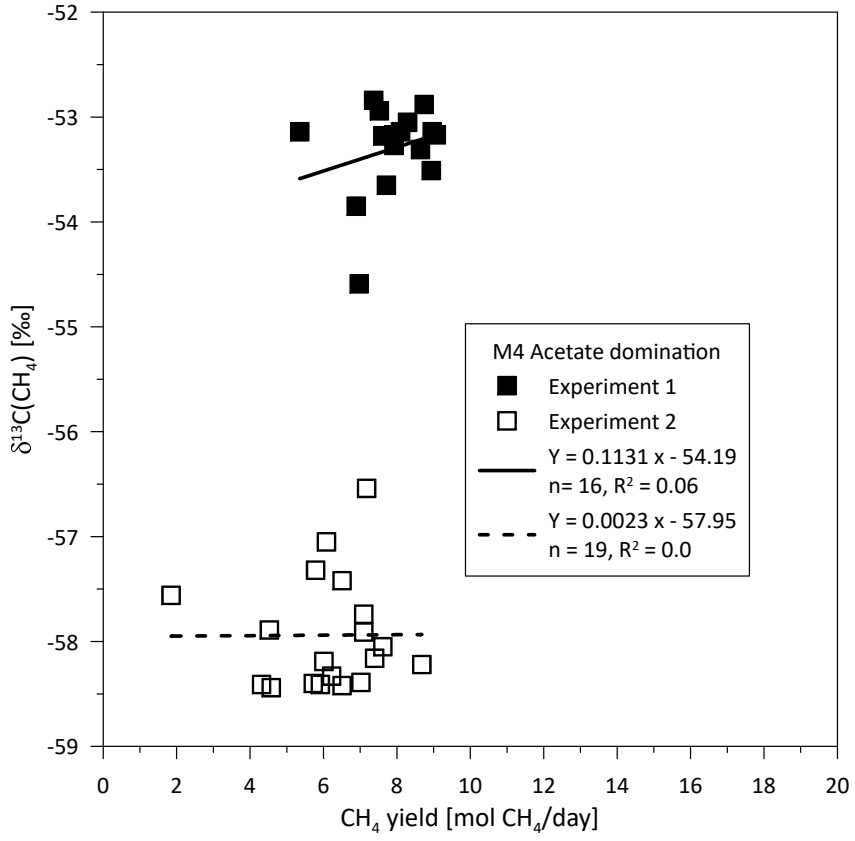


Figure A12. Correlation of $\delta^{13}C(CH_4)$ values and CH_4 yield in Experiment M4 with acetate domination.

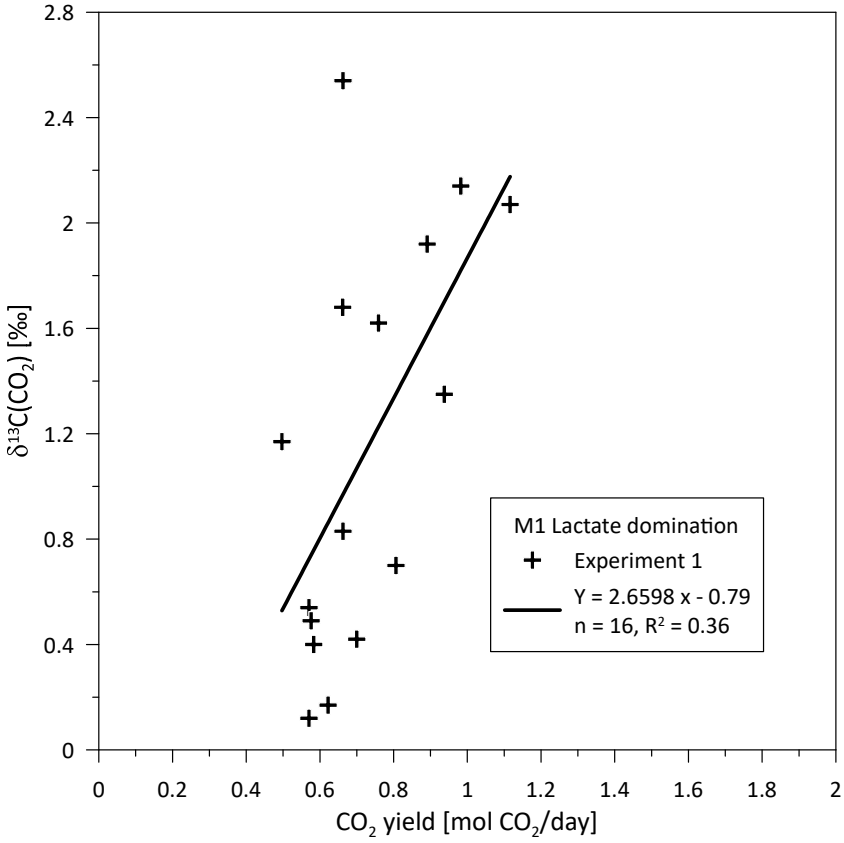


Figure A13. Correlation of $\delta^{13}C(CO_2)$ values and CO_2 yield in Experiment M1 with lactate domination.

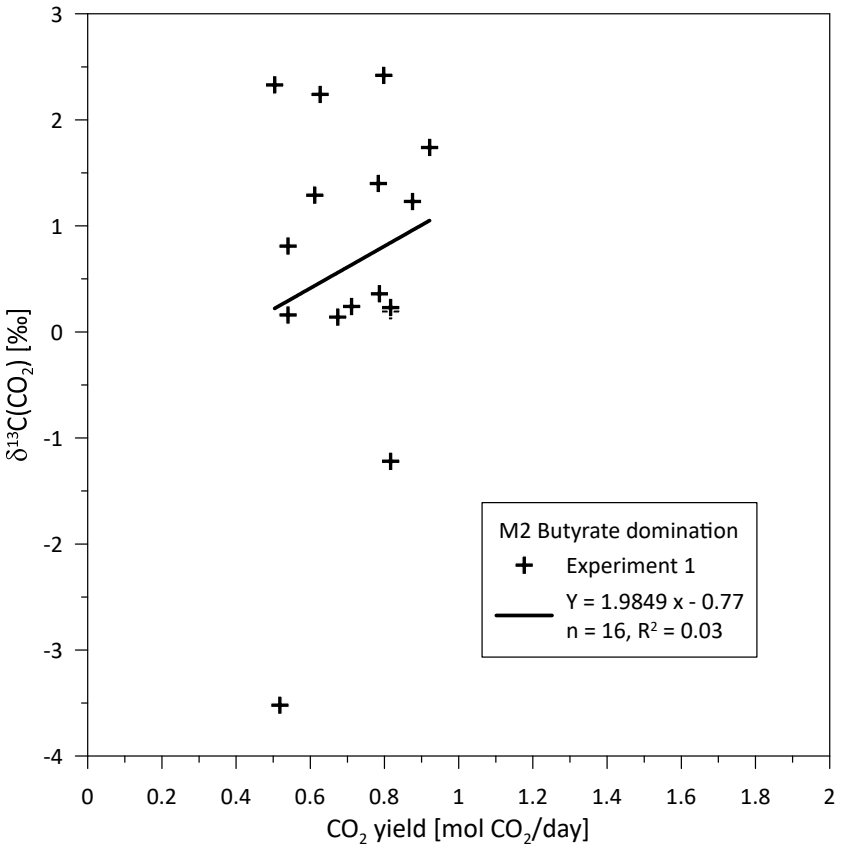


Figure A14. Correlation of $\delta^{13}C(CO_2)$ values and CO_2 yield in Experiment M2 with butyrate domination.

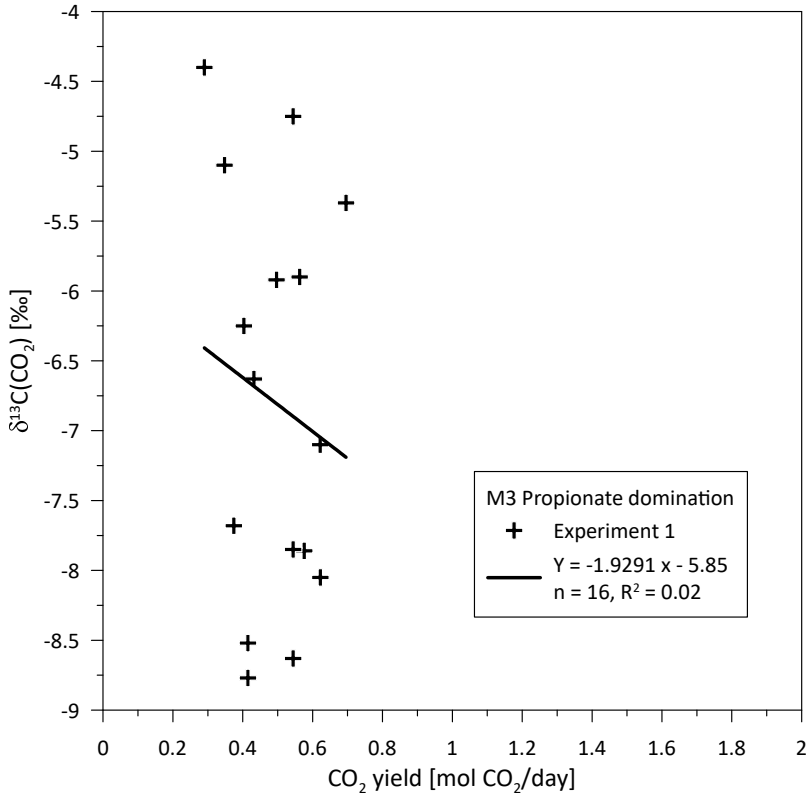


Figure A15. Correlation of $\delta^{13}C(CO_2)$ values and CO_2 yield in Experiment M3 with propionate domination.

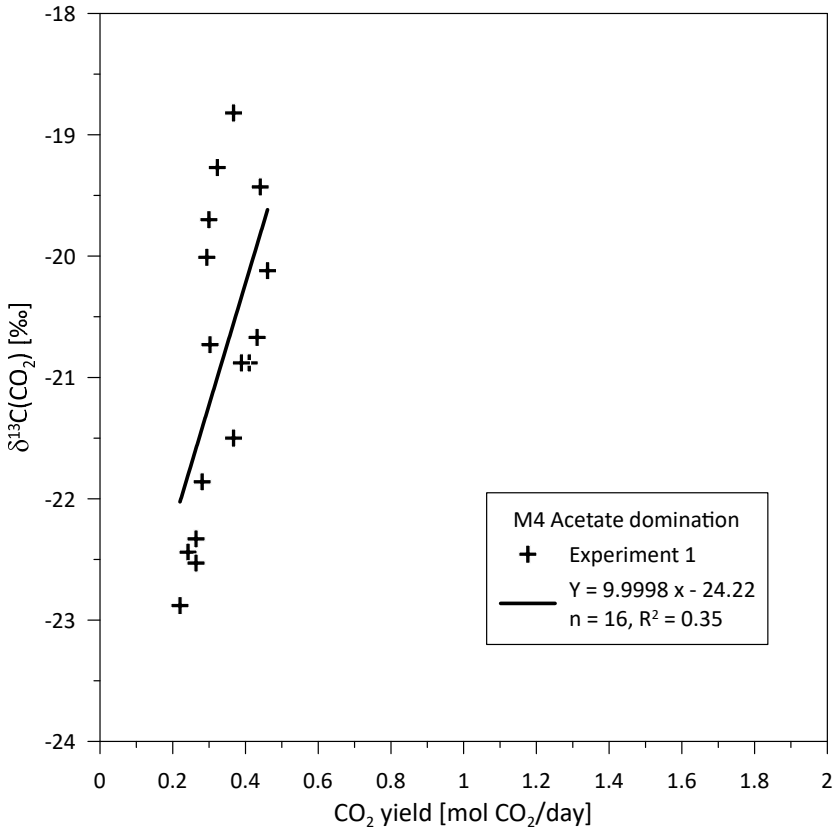


Figure A16. Correlation of $\delta^{13}C(CO_2)$ values and CO_2 yield in Experiment M4 with acetate domination.

Appendix B

The table with the data regarding biogas, DIC, and organic acid concentrations in Experiments 1 and 2.

Table A1. Carbon isotope signatures and biogas production dynamics in bioreactors M1, M2, M3 and M4 during Experiments 1 and 2.

Bioreactor	Time [Day]	$\delta^{13}C(CH_4)$ [‰]	$\delta^{13}C(CO_2)$ [‰]	$\delta^{13}C(DIC)$ [‰]	$\alpha^{13}C_{CO2\text{-}CH4}$	CH_4 [%]	CO_2 [%]	Biogas [dm^3/Day]	CH_4 [dm^3/Day]	CH_4 [mol CH_4/Day]	CO_2 [dm^3 CO_2/Day]	CO_2 [mol CO_2/Day]
M1	709	−39.9	1.7	9.2	1.0433	60	27	2.5	1.5	6.6	0.7	3.0
M1	711	−39.4	1.2	n.a.	1.0422	62	23	2.2	1.3	6.0	0.5	2.2
M1	714	−39.3	0.4	7.8	1.0413	72	27	2.2	1.6	6.9	0.6	2.6
M1	716	−40.6	0.4	n.a.	1.0427	73	27	2.6	1.9	8.4	0.7	3.1
M1	718	−40.2	0.1	n.a.	1.0420	71	22	2.6	1.8	8.2	0.6	2.5
M1	721	−39.6	0.2	8.0	1.0414	64	24	2.6	1.7	7.4	0.6	2.8
M1	723	−39.7	0.5	n.a.	1.0418	62	22	2.6	1.6	7.2	0.6	2.5
M1	725	−39.9	0.7	n.a.	1.0423	60	28	2.9	1.7	7.7	0.8	3.6
M1	728	−39.9	0.8	7.9	1.0425	75	23	2.9	2.2	9.6	0.7	3.0
M1	730	−39.1	0.5	n.a.	1.0412	77	20	2.9	2.2	9.9	0.6	2.6
M1	732	−40.0	1.4	n.a.	1.0430	74	21	4.5	3.3	14.7	0.9	4.2
M1	735	−40.6	2.1	9.6	1.0446	73	22	4.5	3.3	14.5	1.0	4.4
M1	738	−41.7	2.1	n.a.	1.0457	72	25	4.5	3.2	14.3	1.1	5.0
M1	742	−42.2	2.5	9.8	1.0467	80	20	3.3	2.6	11.8	0.7	3.0
M1	744	n.a.	n.a.	n.a.	n.a.	72	22	3.3	2.4	10.6	0.7	3.3
M1	746	−41.1	1.6	n.a.	1.0446	76	23	3.3	2.5	11.2	0.8	3.4
M1	749	−41.2	1.9	9.4	1.0449	67	27	3.3	2.2	9.9	0.9	4.0
M1	799	−33.9	1.6	8.6	1.0368	75	n.a.	5.0	3.8	16.9	n.a.	n.a.
M1	803	−35.6	3.2	10.8	1.0402	75	n.a.	5.0	3.8	16.9	n.a.	n.a.
M1	806	−35.2	4.0	11.2	1.0407	62	n.a.	5.0	3.1	14.0	n.a.	n.a.
M1	810	−35.6	4.0	n.a.	1.0411	66	n.a.	4.8	3.2	14.1	n.a.	n.a.
M1	813	−34.9	3.7	10.9	1.0400	68	n.a.	4.8	3.3	14.6	n.a.	n.a.
M1	817	−35.9	3.3	n.a.	1.0406	77	n.a.	4.5	3.5	15.5	n.a.	n.a.
M1	820	−34.8	3.4	10.3	1.0396	71	n.a.	4.5	3.2	14.3	n.a.	n.a.
M1	824	−35.8	4.0	n.a.	1.0413	78	n.a.	3.6	2.8	12.5	n.a.	n.a.
M1	827	−35.4	3.9	10.8	1.0408	73	n.a.	3.6	2.6	11.7	n.a.	n.a.
M1	831	−36.7	4.1	n.a.	1.0424	72	n.a.	2.7	1.9	8.7	n.a.	n.a.
M1	834	−35.4	4.0	10.8	1.0408	72	n.a.	2.7	1.9	8.7	n.a.	n.a.
M1	839	−36.0	3.8	n.a.	1.0413	72	n.a.	3.2	2.3	10.3	n.a.	n.a.
M1	841	−36.2	4.0	10.7	1.0416	72	n.a.	3.2	2.3	10.3	n.a.	n.a.
M1	845	−36.8	4.1	n.a.	1.0424	73	n.a.	2.6	1.9	8.5	n.a.	n.a.
M1	848	−37.2	4.9	10.8	1.0438	72	n.a.	2.6	1.9	8.4	n.a.	n.a.
M1	852	−37.1	4.9	n.a.	1.0437	76	n.a.	3.0	2.3	10.2	n.a.	n.a.
M1	855	−37.7	4.8	11.8	1.0442	78	n.a.	3.0	2.3	10.4	n.a.	n.a.
M1	859	−38.3	5.3	n.a.	1.0453	70	n.a.	3.6	2.5	11.3	n.a.	n.a.
M1	862	−39.1	5.6	10.8	1.0465	73	n.a.	3.6	2.6	11.7	n.a.	n.a.
M1	866	−36.0	5.9	n.a.	1.0435	76	n.a.	3.3	2.5	11.2	n.a.	n.a.
M1	869	n.a.	n.a.	n.a.	n.a.	86	n.a.	3.3	2.8	12.7	n.a.	n.a.
M1	873	n.a.	n.a.	n.a.	n.a.	76	n.a.	2.3	1.7	7.8	n.a.	n.a.
M1	876	n.a.	n.a.	n.a.	n.a.	77	n.a.	2.3	1.8	7.9	n.a.	n.a.

Table A1. *Cont.*

Bioreactor	Time [Day]	$\delta^{13}C(CH_4)$ [‰]	$\delta^{13}C(CO_2)$ [‰]	$\delta^{13}C(DIC)$ [‰]	$\alpha^{13}C_{CO2\text{-}CH4}$	CH_4 [%]	CO_2 [%]	Biogas [dm^3/Day]	CH_4 [dm^3/Day]	CH_4 [mol CH_4/Day]	CO_2 [dm^3 CO_2/Day]	CO_2 [mol CO_2/Day]
M1	881	n.a.	n.a.	n.a.	n.a.	74	n.a.	3.2	2.4	10.6	n.a.	n.a.
M2	709	−49.2	−3.5	4.4	1.0480	70	14	3.7	2.6	11.6	0.5	2.3
M2	711	−47.7	−1.2	n.a.	1.0488	75	21	3.9	2.9	13.0	0.8	3.6
M2	714	−46.3	0.2	8.1	1.0488	77	21	3.9	3.0	13.4	0.8	3.6
M2	716	−46.3	0.2	n.a.	1.0488	78	21	3.9	3.0	13.5	0.8	3.6
M2	718	−45.9	0.2	n.a.	1.0483	80	19	3.7	3.0	13.4	0.7	3.2
M2	721	−45.7	0.4	9.2	1.0483	73	21	3.7	2.7	12.2	0.8	3.5
M2	723	−46.1	0.1	n.a.	1.0484	80	18	3.7	3.0	13.4	0.7	3.0
M2	725	−46.4	0.2	n.a.	1.0488	82	15	3.6	3.0	13.2	0.5	2.4
M2	728	−46.2	0.8	8.7	1.0493	82	15	3.6	3.0	13.2	0.5	2.4
M2	730	−46.5	1.3	n.a.	1.0502	83	17	3.6	3.0	13.3	0.6	2.7
M2	732	−46.0	1.7	n.a.	1.0501	80	20	4.6	3.7	16.5	0.9	4.1
M2	735	−45.5	1.2	8.6	1.0490	80	19	4.6	3.7	16.5	0.9	3.9
M2	738	−46.8	1.4	n.a.	1.0505	82	17	4.6	3.8	16.9	0.8	3.5
M2	742	−46.8	2.2	10.9	1.0515	84	15	4.2	3.5	15.7	0.6	2.8
M2	744	n.a.	n.a.	n.a.	n.a.	85	15	4.2	3.5	15.8	0.6	2.8
M2	746	−47.2	2.4	n.a.	1.0521	77	19	4.2	3.2	14.4	0.8	3.6
M2	749	−46.7	2.3	9.5	1.0515	43	12	4.2	1.8	8.1	0.5	2.3
M2	799	−47.9	0.2	6.8	1.0505	81	n.a.	3.2	2.6	11.5	n.a.	n.a.
M2	803	−46.2	3.2	10.4	1.0518	84	n.a.	3.2	2.7	11.9	n.a.	n.a.
M2	806	−45.8	3.0	10.3	1.0512	78	n.a.	3.2	2.5	11.0	n.a.	n.a.
M2	810	−46.1	3.4	n.a.	1.0519	82	n.a.	3.7	3.1	13.7	n.a.	n.a.
M2	813	−45.4	2.5	8.6	1.0502	81	n.a.	3.7	3.0	13.5	n.a.	n.a.
M2	817	−46.9	4.8	n.a.	1.0542	81	n.a.	4.2	3.4	15.1	n.a.	n.a.
M2	820	−45.7	6.6	14.0	1.0548	78	n.a.	4.2	3.3	14.5	n.a.	n.a.
M2	824	−46.5	4.0	n.a.	1.0529	81	n.a.	3.6	2.9	13.0	n.a.	n.a.
M2	827	−46.1	7.4	15.1	1.0560	81	n.a.	3.6	2.9	13.0	n.a.	n.a.
M2	831	−46.5	6.2	n.a.	1.0553	79	n.a.	2.3	1.8	8.1	n.a.	n.a.
M2	834	−47.1	4.5	12.5	1.0541	77	n.a.	2.3	1.8	7.9	n.a.	n.a.
M2	839	−46.6	7.8	n.a.	1.0570	79	n.a.	2.4	1.9	8.6	n.a.	n.a.
M2	841	−46.1	8.2	15.6	1.0570	79	n.a.	2.4	1.9	8.6	n.a.	n.a.
M2	845	−46.5	8.9	n.a.	1.0580	82	n.a.	2.9	2.4	10.5	n.a.	n.a.
M2	848	−47.1	9.1	16.2	1.0589	83	n.a.	2.9	2.4	10.7	n.a.	n.a.
M2	852	−45.8	10.1	n.a.	1.0586	79	n.a.	2.9	2.3	10.2	n.a.	n.a.
M2	855	−45.4	9.2	17.2	1.0572	75	n.a.	2.9	2.2	9.6	n.a.	n.a.
M2	859	−44.8	8.5	n.a.	1.0558	77	n.a.	2.6	2.0	8.9	n.a.	n.a.
M2	862	−44.9	9.6	15.5	1.0571	76	n.a.	2.6	2.0	8.8	n.a.	n.a.
M2	866	−45.2	9.1	n.a.	1.0569	80	n.a.	3.3	2.6	11.8	n.a.	n.a.
M2	869	−44.8	10.1	16.0	1.0575	76	n.a.	3.3	2.5	11.2	n.a.	n.a.
M2	876	−47.0	9.2	16.8	1.0590	73	n.a.	3.0	2.2	9.9	n.a.	n.a.
M3	709	−50.9	−7.1	0.8	1.0461	68	24	2.6	1.8	7.9	0.6	2.8
M3	711	−50.0	−7.9	n.a.	1.0444	73	25	2.3	1.7	7.5	0.6	2.6
M3	714	−50.4	−8.8	−0.9	1.0438	81	18	2.3	1.9	8.3	0.4	1.9
M3	716	−50.0	−8.5	n.a.	1.0437	81	18	2.3	1.9	8.3	0.4	1.9

Table A1. *Cont.*

Bioreactor	Time [Day]	$\delta^{13}C(CH_4)$ [‰]	$\delta^{13}C(CO_2)$ [‰]	$\delta^{13}C(DIC)$ [‰]	$\alpha^{13}C_{CO2\text{-}CH4}$	CH_4 [%]	CO_2 [%]	Biogas [dm^3/Day]	CH_4 [dm^3/Day]	CH_4 [mol CH_4/Day]	CO_2 [dm^3 CO_2/Day]	CO_2 [mol CO_2/Day]
M3	718	−50.2	−8.6	n.a.	1.0437	83	14	3.9	3.2	14.4	0.5	2.4
M3	721	−50.3	−8.1	−0.3	1.0445	73	16	3.9	2.8	12.7	0.6	2.8
M3	723	−50.1	−7.9	n.a.	1.0444	78	14	3.9	3.0	13.5	0.5	2.4
M3	725	−50.4	−7.7	n.a.	1.0450	80	13	2.9	2.3	10.3	0.4	1.7
M3	728	−51.1	−6.6	0.8	1.0468	82	15	2.9	2.4	10.5	0.4	1.9
M3	730	−50.6	−6.3	n.a.	1.0467	86	14	2.9	2.5	11.1	0.4	1.8
M3	732	−51.3	−5.9	n.a.	1.0479	80	17	3.3	2.6	11.8	0.6	2.5
M3	735	−51.4	−5.4	2.6	1.0486	78	21	3.3	2.6	11.5	0.7	3.1
M3	738	−51.7	−5.9	n.a.	1.0483	59	15	3.3	2.0	8.7	0.5	2.2
M3	742	−52.1	−4.8	2.8	1.0500	79	21	2.6	2.0	9.1	0.5	2.4
M3	744	n.a.	n.a.	n.a.	n.a.	83	17	2.6	2.2	9.6	0.4	2.0
M3	746	−52.7	−5.1	n.a.	1.0503	76	12	2.9	2.2	9.8	0.3	1.6
M3	749	−52.5	−4.4	2.9	1.0508	75	10	2.9	2.2	9.7	0.3	1.3
M3	799	−53.8	−7.0	0.6	1.0495	83	n.a.	2.4	2.0	9.1	n.a.	n.a.
M3	803	−54.9	−9.0	−1.2	1.0487	89	n.a.	2.4	2.2	9.7	n.a.	n.a.
M3	806	−55.6	−9.3	−1.7	1.0490	81	n.a.	2.4	2.0	8.9	n.a.	n.a.
M3	810	−56.4	−7.7	n.a.	1.0516	82	n.a.	2.4	2.0	9.0	n.a.	n.a.
M3	813	−56.0	−7.1	−0.3	1.0518	82	n.a.	2.4	2.0	9.0	n.a.	n.a.
M3	817	−56.2	−7.3	n.a.	1.0517	84	n.a.	2.2	1.8	8.1	n.a.	n.a.
M3	820	−56.0	−7.4	−0.5	1.0514	82	n.a.	2.2	1.8	7.9	n.a.	n.a.
M3	824	−56.8	−5.9	n.a.	1.0539	85	n.a.	1.9	1.6	7.3	n.a.	n.a.
M3	827	−56.9	−5.8	1.0	1.0542	86	n.a.	1.9	1.6	7.4	n.a.	n.a.
M3	831	−57.3	−5.4	n.a.	1.0550	85	n.a.	2.6	2.2	9.8	n.a.	n.a.
M3	834	−57.2	−4.8	1.1	1.0556	82	n.a.	2.6	2.1	9.5	n.a.	n.a.
M3	839	−57.4	−5.8	n.a.	1.0547	72	n.a.	2.7	2.0	8.8	n.a.	n.a.
M3	841	−57.1	−4.2	1.7	1.0561	85	n.a.	2.7	2.3	10.4	n.a.	n.a.
M3	845	−57.3	−4.3	n.a.	1.0562	85	n.a.	2.4	2.1	9.3	n.a.	n.a.
M3	848	−57.8	−4.2	1.7	1.0569	85	n.a.	2.4	2.1	9.3	n.a.	n.a.
M3	852	−58.3	−3.8	n.a.	1.0578	84	n.a.	2.6	2.2	9.7	n.a.	n.a.
M3	855	−58.6	−3.3	3.1	1.0587	85	n.a.	2.6	2.2	9.8	n.a.	n.a.
M3	859	−58.8	−2.7	n.a.	1.0596	83	n.a.	3.0	2.5	11.2	n.a.	n.a.
M3	862	−58.3	−2.6	4.1	1.0591	83	n.a.	3.0	2.5	11.2	n.a.	n.a.
M3	866	n.a.	n.a.	n.a.	n.a.	85	n.a.	2.4	2.1	9.3	n.a.	n.a.
M3	869	−58.0	−2.9	3.5	1.0584	85	n.a.	2.4	2.1	9.3	n.a.	n.a.
M3	873	n.a.	n.a.	n.a.	n.a.	85	n.a.	2.7	2.3	10.4	n.a.	n.a.
M3	876	n.a.	n.a.	n.a.	n.a.	87	n.a.	2.7	2.4	10.6	n.a.	n.a.
M3	881	n.a.	n.a.	n.a.	n.a.	89	n.a.	3.7	3.3	14.9	n.a.	n.a.
M4	709	−54.6	−22.4	−15.1	1.0340	71	11	2.2	1.6	7.0	0.2	1.1
M4	711	−52.8	−22.5	n.a.	1.0320	75	12	2.2	1.7	7.4	0.3	1.2
M4	714	−53.5	−22.9	−15.4	1.0324	91	10	2.2	2.0	8.9	0.2	1.0
M4	716	−53.3	−22.3	n.a.	1.0327	88	12	2.2	1.9	8.6	0.3	1.2
M4	718	−53.1	−21.9	n.a.	1.0329	86	13	2.2	1.9	8.3	0.3	1.3
M4	721	−53.2	−21.5	−13.8	1.0334	82	17	2.2	1.8	7.9	0.4	1.6
M4	723	−52.9	−20.7	n.a.	1.0341	78	20	2.2	1.7	7.5	0.4	1.9
M4	725	−53.2	−20.9	n.a.	1.0341	79	19	2.2	1.7	7.6	0.4	1.8

Table A1. *Cont.*

Bioreactor	Time [Day]	$\delta^{13}C(CH_4)$ [‰]	$\delta^{13}C(CO_2)$ [‰]	$\delta^{13}C(DIC)$ [‰]	$\alpha^{13}C_{CO2\text{-}CH4}$	CH_4 [%]	CO_2 [%]	Biogas [dm^3/Day]	CH_4 [dm^3/Day]	CH_4 [mol CH_4/Day]	CO_2 [dm^3 CO_2/Day]	CO_2 [mol CO_2/Day]
M4	728	−53.7	−20.9	−13.6	1.0346	80	18	2.2	1.7	7.7	0.4	1.7
M4	730	−53.1	−20.7	n.a.	1.0342	84	14	2.2	1.8	8.1	0.3	1.4
M4	732	−53.9	−19.7	n.a.	1.0361	67	13	2.3	1.5	6.9	0.3	1.3
M4	735	−53.3	−20.1	−12.9	1.0350	77	20	2.3	1.8	7.9	0.5	2.1
M4	738	−52.9	−19.3	n.a.	1.0355	85	14	2.3	2.0	8.7	0.3	1.4
M4	742	−53.2	−18.8	−11.2	1.0363	83	15	2.4	2.0	9.1	0.4	1.6
M4	744	n.a.	n.a.	n.a.	n.a.	84	14	2.4	2.1	9.2	0.3	1.5
M4	746	−53.1	−19.4	n.a.	1.0356	82	18	2.4	2.0	9.0	0.4	2.0
M4	749	−53.1	−20.0	−12.7	1.0350	49	12	2.4	1.2	5.4	0.3	1.3
M4	799	n.a.	n.a.	n.a.	n.a.	84	n.a.	1.6	1.3	5.9	n.a.	n.a.
M4	803	−57.4	−30.2	−24.0	1.0289	92	n.a.	1.6	1.5	6.5	n.a.	n.a.
M4	806	−57.1	−32.3	−26.4	1.0263	86	n.a.	1.6	1.4	6.1	n.a.	n.a.
M4	810	−57.9	−33.2	n.a.	1.0263	92	n.a.	1.7	1.6	7.1	n.a.	n.a.
M4	813	−57.7	−33.1	−27.5	1.0261	92	n.a.	1.7	1.6	7.1	n.a.	n.a.
M4	817	−58.2	−34.3	n.a.	1.0254	90	n.a.	2.2	1.9	8.7	n.a.	n.a.
M4	820	−58.1	−33.8	−28.5	1.0257	79	n.a.	2.2	1.7	7.6	n.a.	n.a.
M4	824	−57.6	−33.4	n.a.	1.0257	23	n.a.	1.8	0.4	1.8	n.a.	n.a.
M4	827	−58.2	−32.6	−27.8	1.0272	92	n.a.	1.8	1.7	7.4	n.a.	n.a.
M4	831	−58.4	−33.9	n.a.	1.0260	89	n.a.	1.2	1.0	4.6	n.a.	n.a.
M4	834	−57.9	−34.1	−28.3	1.0253	88	n.a.	1.2	1.0	4.5	n.a.	n.a.
M4	839	−58.4	−34.5	n.a.	1.0254	61	n.a.	1.6	1.0	4.3	n.a.	n.a.
M4	841	−58.2	−34.0	−28.9	1.0257	85	n.a.	1.6	1.3	6.0	n.a.	n.a.
M4	845	−56.5	−33.5	n.a.	1.0245	93	n.a.	1.7	1.6	7.2	n.a.	n.a.
M4	848	−58.4	−33.9	−28.1	1.0260	91	n.a.	1.7	1.6	7.0	n.a.	n.a.
M4	852	−58.3	−34.0	n.a.	1.0258	88	n.a.	1.6	1.4	6.2	n.a.	n.a.
M4	855	−58.4	−34.2	−28.7	1.0257	92	n.a.	1.6	1.5	6.5	n.a.	n.a.
M4	859	−58.4	−34.4	n.a.	1.0255	89	n.a.	1.4	1.3	5.7	n.a.	n.a.
M4	862	−58.4	−33.6	−27.5	1.0264	92	n.a.	1.4	1.3	5.9	n.a.	n.a.
M4	866	−57.3	−32.4	n.a.	1.0264	90	n.a.	1.4	1.3	5.8	n.a.	n.a.
M4	869	n.a.	n.a.	n.a.	n.a.	80	n.a.	1.4	1.2	5.1	n.a.	n.a.
M4	873	n.a.	n.a.	n.a.	n.a.	79	n.a.	1.3	1.0	4.6	n.a.	n.a.
M4	876	n.a.	n.a.	n.a.	n.a.	92	n.a.	1.3	1.2	5.3	n.a.	n.a.
M4	881	n.a.	n.a.	n.a.	n.a.	90	n.a.	2.2	1.9	8.7	n.a.	n.a.

n.a.—not analysed.

Table A2. Concentrations of organic acids in bioreactors M1, M2, M3 and M4 during Experiments 1 and 2.

Bioreactor	Time [Day]	Lactic Acid [mM/L]	Butyric Acid [mM/L]	Propionic Acid [mM/L]	Acetic Acid [mM/L]
M1	707	0.0	0.0	0.3	0.4
M1	714	0.0	1.3	7.0	8.6
M1	721	0.0	2.0	8.8	10.9
M1	728	0.0	1.1	9.1	11.2
M1	735	1.4	2.8	20.8	25.7
M1	742	0.0	1.6	16.0	19.7
M1	749	0.1	1.5	15.9	19.6

Table A2. *Cont.*

Bioreactor	Time [Day]	Lactic Acid [mM/L]	Butyric Acid [mM/L]	Propionic Acid [mM/L]	Acetic Acid [mM/L]
M1	798	0.1	1.8	20.1	24.7
M1	806	0.0	0.2	12.8	15.8
M1	813	0.0	0.3	13.8	17.0
M1	820	0.0	0.2	12.5	15.4
M1	827	0.0	0.6	15.8	19.5
M1	837	1.1	0.7	17.1	21.1
M1	841	1.1	1.0	20.2	24.9
M1	848	1.1	0.7	14.0	17.2
M1	855	1.1	0.9	24.0	29.6
M1	862	1.1	1.1	19.7	24.3
M1	874	1.1	0.8	14.9	18.4
M1	876	0.0	0.9	20.0	24.6
M1	881	0.0	0.0	13.7	17.0
M2	714	0.0	3.6	8.5	10.5
M2	721	0.0	6.0	20.9	25.8
M2	728	0.0	6.7	21.6	26.7
M2	735	0.1	10.0	40.5	49.9
M2	742	0.1	11.7	39.0	48.2
M2	749	0.0	6.0	31.6	38.9
M2	798	0.1	6.1	8.2	10.1
M2	806	0.0	5.4	32.9	40.5
M2	813	0.0	6.0	36.1	44.6
M2	820	0.0	7.3	34.8	43.0
M2	827	0.0	18.5	68.7	84.7
M2	837	0.0	14.6	66.9	82.5
M2	841	1.1	17.0	76.3	94.1
M2	848	0.0	7.9	39.1	48.2
M2	855	0.0	13.3	94.1	116.1
M2	862	0.0	7.5	45.4	56.1
M2	874	0.0	14.4	89.4	110.3
M2	876	0.0	11.3	56.9	70.2
M2	881	0.0	8.9	55.8	68.9
M3	707	0.0	0.0	1.1	1.4
M3	714	0.0	1.6	10.6	13.1
M3	721	0.0	1.5	12.2	15.0
M3	728	0.0	0.7	9.5	11.7
M3	735	0.1	1.1	20.4	25.1
M3	742	0.0	0.7	13.8	17.1
M3	749	0.1	1.1	24.7	30.5
M3	798	0.1	0.4	8.4	10.4
M3	806	0.0	0.3	14.2	17.5
M3	813	0.0	0.3	14.0	17.3
M3	820	0.0	1.1	27.7	34.2
M3	827	0.0	0.9	25.2	31.1
M3	837	1.1	0.7	28.9	35.6
M3	841	0.0	1.0	27.5	33.9
M3	848	0.0	0.7	24.1	29.8
M3	855	0.0	0.8	33.2	41.0
M3	862	0.0	0.7	20.0	24.7
M3	874	0.0	0.8	37.5	46.3
M3	876	0.0	0.8	27.3	33.6
M3	881	0.0	0.6	17.1	21.1
M4	707	0.0	0.0	0.8	1.0
M4	714	0.0	0.7	11.9	14.7
M4	728	0.0	0.8	13.9	17.1
M4	735	0.1	2.5	26.0	32.1
M4	742	0.1	2.2	22.7	28.1
M4	749	0.0	1.8	25.2	31.1
M4	798	0.0	0.1	10.0	12.3
M4	806	0.0	0.1	24.3	30.0

Table A2. *Cont.*

Bioreactor	Time [Day]	Lactic Acid [mM/L]	Butyric Acid [mM/L]	Propionic Acid [mM/L]	Acetic Acid [mM/L]
M4	813	0.0	0.1	23.8	29.4
M4	820	0.0	0.6	22.0	27.2
M4	827	0.0	0.6	37.1	45.8
M4	837	1.1	0.5	28.8	35.6
M4	841	0.0	0.0	33.3	41.0
M4	848	0.0	0.0	24.0	29.6
M4	855	0.0	0.5	36.5	45.1
M4	862	0.0	0.7	26.0	32.1
M4	874	0.0	0.5	15.3	18.9
M4	876	0.0	0.0	19.1	23.5
M4	881	0.0	0.0	20.8	25.7

References

1. Bao, Y.; Li, D.; Ju, Y. Constraints of biomethane generation yield and carbon isotope fractionation effect in the pathway of acetotrophic with different coal-rank coals. *Fuel* **2021**, *305*, 121493. [CrossRef]
2. Chanton, J.P. The effect of gas transport mechanism on the isotope signature of methane in wetlands. *Org. Geochem.* **2005**, *36*, 753–768. [CrossRef]
3. Fey, A.; Claus, P.; Conrad, R. Temporal change of ^{13}C isotope signatures and methanogenic pathways in rice field soil incubated anoxically at different temperatures. *Geochim. Cosmochim. Acta* **2004**, *68*, 293–306. [CrossRef]
4. Gruca-Rokosz, R.; Koszelnik, P. Production pathways for CH_4 and CO_2 in sediments of two freshwater ecosystems in south-eastern Poland. *PLoS ONE* **2018**, *13*, e0199755. [CrossRef] [PubMed]
5. Szafranek-Nakonieczna, A.; Zheng, Y.; Słowakiewicz, M.; Pytlak, A.; Polakowski, C.; Kubaczyński, A.; Bieganowski, A.; Banach, A.; Wolińska, A.; Stępniewska, Z. Methanogenic potential of lignites in Poland. *Int. J. Coal Geol.* **2018**, *196*, 201–210. [CrossRef]
6. Mayumi, D.; Mochimaru, H.; Tamaki, H.; Yamamoto, K.; Yoshioka, H.; Suzuki, Y.; Kamagata, Y.; Sakata, S. Methane production from coal by a single methanogen. *Science* **2016**, *354*, 222–225. [CrossRef] [PubMed]
7. Woszczyk, M.; Kotarba, M.J.; Whiticar, M.; Schubert, C. Processes affecting molecular and stable isotope compositions of sediment gas in estuarine waters along the southern Baltic coast (Poland). *Biogeochemistry* **2016**, *131*, 203–228. [CrossRef]
8. Milkov, A.V.; Etiope, G. Revised genetic diagrams for natural gases based on a global dataset of >20,000 samples. *Org. Geochem.* **2018**, *125*, 109–120. [CrossRef]
9. Sherwood Lollar, B.; Lacrampe-Coulome, G.; Slater, G.F.; Ward, J.; Moser, D.P.; Gihring, T.M.; Lin, L.H.; Onstott, T.C. Unravelling abiogenic and biogenic sources of methane in the Earth's deep subsurface. *Chem. Geol.* **2006**, *226*, 328–339. [CrossRef]
10. Stams, A.J.; Plugge, C.M. Electron transfer in syntrophic communities of anaerobic bacteria and archea. *Nat. Rev. Microbiol.* **2009**, *7*, 568–577. [CrossRef] [PubMed]
11. Clark, I.D.; Fritz, P. *Environmental Isotopes in Hydrogeology*; CRC Press: Boca Raton, FL, USA, 1997.
12. Tullner, M.; Centler, F.; Richnow, H.H.; Fischer, A. Quantification of organic pollutant degradation in contaminated aquifers using compound specific stable isotope analysis—Review of recent developments. *Org. Geochem.* **2012**, *42*, 1440–1460. [CrossRef]
13. Hoefs, J. *Stable Isotope Geochemistry*, 6th ed.; Springer: Berlin, Heidelberg, 2009.
14. Sharp, Z. *Principles of Stable Isotope Geochemistry*, 2nd ed.; University of New Mexico: Albuquerque, New Mexico, 2017. [CrossRef]
15. Blair, N.E.; Carter, W.D. The carbon isotope biogeochemistry of acetate from a methanogenic marine sediment. *Geochim. Cosmochim. Acta* **1992**, *56*, 1247–1258. [CrossRef]
16. Sugimoto, A.; Wada, E. Carbon isotopic composition of bacterial methane in a soil incubation experiment: Contributions of acetate and CO_2/H_2. *Geochim. Cosmochim. Acta* **1993**, *57*, 4015–4027. [CrossRef]
17. Conrad, R. Quantification of methanogenic pathways using stable carbon isotopic signatures: A review and a proposal. *Org. Geochem.* **2005**, *36*, 739–752. [CrossRef]
18. Whiticar, M.J. Carbon and hydrogen isotope systematics of bacterial formation and oxidation of methane. *Chem. Geol.* **1999**, *161*, 291–314. [CrossRef]
19. Zinder, S.H. Physiological ecology of methanogens. In *Methanogenesis: Ecology, Physiology, Biochemistry and Genetics*; Ferry, J.G., Ed.; Chapman and Hall: New York, NY, USA, 1993; pp. 128–206.
20. Gruca-Rokosz, R.; Szal, D.; Bartoszek, L.; Pekala, A. Isotopic evidence for vertical diversification of methane production pathways in freshwater sediments of Nielisz reservoir (Poland). *Catena* **2020**, *195*, 104803. [CrossRef]
21. Corbett, J.E.; Tfaily, M.; Burdige, D.; Cooper, W.; Glaser, P.; Chanton, J.P. Partitioning pathways of CO_2 production in peatlands with stable carbon isotopes. *Biogeochemistry* **2013**, *114*, 327–340. [CrossRef]

22. Blair, N.E.; Aller, R.C. Anaerobic methane oxidation on the Amazon shelf. *Geochim. Cosmochim. Acta* **1995**, *59*, 3707–3715. [CrossRef]
23. Martens, C.S.; Albert, D.B.; Alperin, M.J. Stable isotope tracing of anaerobic methane oxidation in the gassy sediments of Eckernförde Bay German Baltic Sea. *Am. J. Sci.* **1999**, *299*, 589–610. [CrossRef]
24. Botz, R.; Pokojski, H.D.; Schmitt, M.; Thomm, M. Carbon isotope fractionation during bacterial methanogenesis by CO_2 reduction. *Org. Geochem.* **1996**, *25*, 255–262. [CrossRef]
25. Gelwicks, J.T.; Rissati, J.B.; Hayes, J.M. Carbon isotope effects associated with acetoclastic methanogenesis. *Appl. Environ. Microbiol.* **1994**, *60*, 467–472. [CrossRef] [PubMed]
26. Krzycki, J.A.; Kenealy, W.R.; Deniro, M.J.; Zeikus, J.G. Stable isotope carbon fractionation by *Methanosarcina barkeri* during methanogenesis from acetate, methanol or carbon dioxide hydrogen. *Appl. Environ. Microbiol.* **1987**, *53*, 2597–2599. [CrossRef]
27. Whiticar, M.J.; Faber, E.; Schoell, M. Biogenic methane formation in marine and freshwater environments—CO_2 reduction vs. acetate fermentation—Isotopic evidence. *Geochim. Cosmochim. Acta* **1986**, *50*, 693–709. [CrossRef]
28. Freude, C.; Blaser, M. Carbon isotope fractionation during catabolism and anabolism in acetogenic bacteria growing on different substrates. *Appl. Environ. Microbiol.* **2016**, *82*, 2728–2737. [CrossRef] [PubMed]
29. Games, L.N.; Hayes, J.M.; Gunsalus, R.P. Methaneproducing bacteria: Natural fractionations the stable carbon isotopes. *Geochim. Cosmochim. Acta* **1978**, *42*, 1295–1297. [CrossRef]
30. Waldron, S.; Scott, E.M.; Vihermaa, L.E.; Newton, J. Quantifying precision and accuracy of measurements of dissolved inorganic carbon stable isotopic composition using continuous-flow isotope-ratio mass spectrometry. *Rapid Commun. Mass Spectrom.* **2014**, *8*, 1117–1126. [CrossRef] [PubMed]
31. Meister, P.; Reyes, C. The Carbon-Isotope Record of the Sub-Seafloor Biosphere. *Geosciences* **2019**, *9*, 507. [CrossRef]
32. Polag, D.; May, T.; Müller, L.; König, H.; Jacobi, F.; Laukenmann, S.; Keppler, F. Online monitoring of stable carbon isotopes of methane in anaerobic digestion as a new tool for early warning of process instability. *Bioresour. Technol.* **2015**, *197*, 161–170. [CrossRef] [PubMed]
33. Kufka, D.; Bucha, M.; Pleśniak, Ł.; Jędrysek, M.O. Stable isotopes of C and H in methane fermentation of agriculture substrates at different temperature conditions. *Open Geosci.* **2019**, *11*, 471–481. [CrossRef]
34. Pytlak, A.; Szafranek-Nakonieczna, A.; Goraj, W.; Śnieżyńska, I.; Krążała, A.; Banach, A.; Ristović, I.; Słowakiewicz, M.; Stępniewska, Z. A survey of greenhouse gases production in central European lignites. *Sci. Total Environ.* **2021**, *800*, 149551. [CrossRef] [PubMed]
35. Richnow, H.H.; Meckenstock, R.U.; Reitzel, L.A.; Baun, A.; Ledin, A.; Christensen, T.H. In situ biodegradation determined by carbon isotope fractionation of aromatic hydrocarbons in an anaerobic landfill leachate plume (Vejen Denmark). *J. Contam. Hydrol.* **2003**, *64*, 59–72. [CrossRef] [PubMed]
36. Harirchi, S.; Wainaina, S.; Sar, T.; Nojoumi, S.A.; Parchami, M.; Parchami, M.; Khanal, S.A.; Wong, J.; Awasthi, M.K.; Taerzadeh, M. Microbiological insight into anaerobic digestion for biogas, hydrogen or volatile fatty acids (VFAs): A review. *Bioengineered* **2021**, *13*, 6521–6557. [CrossRef] [PubMed]
37. Detman, A.; Mielecki, D.; Pleśniak, Ł.; Bucha, M.; Janiga, M.; Matyasik, I.; Chojnacka, A.; Jędrysek, M.O.; Błaszczyk, M.K.; Sikora, A. Methane-yielding microbial communities processing lactate-rich substrates: A piece of the anaerobic digestion puzzle. *Biotechnol. Biofuels* **2018**, *11*, 116. [CrossRef] [PubMed]
38. Ghiotto, G.; Detman-Ignatowska, A.; Chojnacka, A.; Orellana, E.; de Bernardini, N.; Fraulini, S.; Treu, L.; Sikora, A.; Campanaro, S. Decipher syntrophies within C2-C4 organic acids degrading anaerobic microbiomes: A multi-omic exploration. *Chem. Eng. J.* **2024**, *489*, 151390. [CrossRef]
39. *ISO 15705:2002*; Water Quality—Determination of the Chemical Oxygen Demand Index (ST-COD)—Small-Scale Sealed-Tube Method. ISO: Geneva, Switzerland, 2002.
40. Detman, A.; Bucha, M.; Treu, L.; Chojnacka, A.; Pleśniak, Ł.; Salamon, A.; Łupikasza, E.; Gromadka, R.; Gawor, J.; Gromadka, A.; et al. Evaluation of acidogenesis products' effect on biogas production performed with metagenomics and isotopic approaches. *Biotechnol. Biofuels* **2021**, *14*, 125. [CrossRef] [PubMed]
41. Paul, D.; Skrzypek, G.; Fórizs, I. Normalization of measured stable isotopic compositions to isotope reference scales—A review. *Rapid Commun. Mass Spectrom.* **2007**, *21*, 3006–3014. [CrossRef] [PubMed]
42. Skrzypek, G.; Sadler, R.; Paul, D. Error propagation in normalization of stable isotope data: A Monte Carlo analysis. *Rapid Commun. Mass Spectrom.* **2010**, *24*, 2697–2705. [CrossRef] [PubMed]
43. Oyekoloa, O.O.; van Hille, R.P.; Harrison, S.T.L. Study of anaerobic lactate metabolism under biosulfidogenic conditions. *Water Res.* **2009**, *43*, 3345–3354. [CrossRef] [PubMed]
44. Alperin, M.J.; Reeburgh, W.S.; Whiticar, M.J. Carbon and hydrogen isotope fractionation resulting from anaerobic methane oxidation. *Glob. Biogeochem. Cycles* **1988**, *2*, 279–288. [CrossRef]
45. Barker, J.F.; Fritz, P. Carbon isotope fractionation during microbial methane oxidation. *Nature* **1981**, *293*, 245–250. [CrossRef]

46. Bucha, M.; Jędrysek, M.O.; Kufka, D.; Pleśniak, Ł.; Marynowski, L.; Kubiak, K.; Błaszczyk, M. Methanogenic fermentation of lignite with carbon-bearing additives, inferred from stable carbon and hydrogen isotopes. *Int. J. Coal Geol.* **2018**, *186*, 65–79. [CrossRef]
47. Bucha, M.; Detman, A.; Pleśniak, Ł.; Drzewicki, W.; Kufka, D.; Chojnacka, A.; Mielecki, D.; Krajniak, J.; Jędrysek, M.O.; Sikora, A.; et al. Microbial methane formation from different lithotypes of Miocene lignites from the Konin Basin, Poland: Geochemistry of the gases and composition of the microbial communities. *Int. J. Coal Geol.* **2020**, *229*, 103558. [CrossRef]
48. Lloyd, M.K.; Trembath-Reichert, E.; Dawson, K.S.; Feakins, S.J.; Mastalerz, M.; Orphan, V.J.; Sessions, A.L.; Eiler, J.M. Methoxyl stable isotopic constraints on the origins and limits of coal-bed methane. *Science* **2021**, *374*, 894–897. [CrossRef] [PubMed]
49. Biega, B. Analysis of the Selected Agricultural Substrates and Food Waste Methane Fermentation Process and Evaluation of the of Biogas Energy Using Possibilities (In English) (Original Title Fermentacja Metanowa Wybranych Substratów Pochodzenia Rolno-Spożywczego: Analiza Warunków Procesu i Możliwości Energetycznego Wykorzystania Biogazu (In Polish)). Doctoral Dissertation, University of Wroclaw, Wrocław, Poland, 2019.
50. Thulner, M.; Fischer, A.; Richnow, H.H.; Wick, L.Y. Influence of mass transfer on stable isotope fractionation. *Appl. Microbiol. Biotechnol.* **2012**, *97*, 441–452. [CrossRef] [PubMed]
51. Lewicki, P.; Lewicka-Szczebak, D.; Skrzypek, G. FRAME—Monte Carlo model for evaluation of the stable isotope mixing and fractionation. *PLoS ONE* **2022**, *17*, e0277204. [CrossRef] [PubMed]

Disclaimer/Publisher's Note: The statements, opinions and data contained in all publications are solely those of the individual author(s) and contributor(s) and not of MDPI and/or the editor(s). MDPI and/or the editor(s) disclaim responsibility for any injury to people or property resulting from any ideas, methods, instructions or products referred to in the content.